Chapter 3. Analysis of protein conformation

3.1 Introduction

In the work presented in the previous chapter, unnatural amino acids were used to make more subtle side chain perturbations than are possible using conventional mutagenesis. However, the range of side chain substitution permitted by the ribosome allows for unnatural amino acids which induce much more radical transformations. In this chapter, nonsense suppression has been used to chemically modify proteins both dynamically and after isolation from the membrane. In the first case, nitrophenylglycine (Npg) was introduced in order to photolytically cleave the polypeptide backbone at the site of the amino acid's introduction.[1] The second set of experiments examined the possibility of site-specific photoinduced cross-linking mediated by the unnatural amino acid benzoylphenylalanine (Bpa).[2] In the third study, hydroxy acids were inserted into the backbone by nonsense suppression.[3-5] The resulting ester linkage is labile to treatment with strong base, which allows for the incorporation of hydroxy acids to be used for mapping protein connectivity.[4] Finally, cysteine and tyrosine residues with bulky photo-removable protecting groups were used to induce conformational changes in a sensitive transmembrane region of the nAChR.[6]

3.2 Site-specific backbone cleavage in nAChR Cys loop using Npg

3.2.1 Site-specific nitrobenzyl-induced photochemical proteolysis (SNIPP)

Site-specific proteolysis is a fundamental step in a wide variety of biological processes.[7] A number of them have become widely publicized because of their role in

human disease.[8] Protease inhibitors for angiotensin-converting enzyme and HIV protease, for example, are highly successful drugs.[9] Targeted proteolysis is typically used at the protein level to activate an enzyme by removing a regulatory domain which holds the proenzyme in check.[10] Among the many examples of this kind of regulation are the caspases, tightly regulated proteases which initiate and carry out the proteolytic steps leading to apoptotic cell death. At the peptide level, potent peptide hormones are synthesized as much larger polypeptides and released by cleavage into their active fragments. As previously mentioned, angiotensin is released this way into the bloodstream. Proteolysis also has a role in certain kinds of pathology. The apparently pathogenic Aβ fragment in Alzheimer's disease is produced by aberrant proteolysis of a precursor protein.[11] A final strategy for proteolytic regulation has been only recently recognized. The protease-activated receptors are thought to be involved in pain pathways, and thus are an increasingly recognized target for clinical intervention.[12] These G-protein-coupled receptors are activated only upon cleavage of an extracellular N-terminal domain.

The ability to site-specifically cleave DNA revolutionized the practice of modern biology. It remains to be seen whether or not site-specific protein cleavage will have such a great effect. The most widespread method of experimental site-specific cleavage is to introduce a protease site into the primary sequence of the protein. This strategy has been used to good effect in structural biology, where proteins may be purified by attached affinity tags, which can then be proteolytically removed to allow characterization of a more native protein.[13] However, *in situ* studies which rely on proteolysis are more difficult, since the proteases responsible for inducing the cleavage can be only under

partial experimental control, at best. Attempts have been made to adapt strategies which have been successful for nucleic acids. Molecules which bind specific DNA sequences have been conjugated to metals or photo-excitable compounds, so that radicals induced by these adducts may cleave the polyphosphate backbone.[14] A similar, though non-specific, strategy has been employed by Daniel Jay to hydrolyze proteins in the vicinity of an irradiated malachite green-conjugated antibody.[15] This technique is known as CALI, or chromophore-assisted laser inactivation.[16] The laboratory of C. V. Kumar has recently introduced a more specific technique for inducing proteolysis this way.[17] Here, dyes are used which bind, under some circumstances, specifically to a given region of a protein. Photolysis of the complex may produce radicals which cleave the backbone.[18,19]

The first general strategy for dynamically cleaving peptide backbones in functioning proteins was only recently introduced. This approach relies on the incorporation of the unnatural amino acid Npg via nonsense suppression. Photolysis induces proton abstraction from the alpha carbon of the amino acid, leading ultimately to hydrolysis.[1] (Figure 3.1)

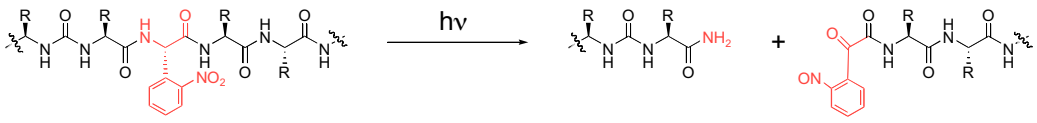

Figure 3.1 Mechanism of SNIPP - backbone cleavage induced by the photolysis of a protein containing a nitrophenylglycine (Npg) residue.[1]

In this initial report, both transmembrane regions and intracellular protein domains were cleaved photolytically in functioning receptors in living cells. A more recent, although less generally useful, derivative of this technique has also been reported, wherein allyl glycine is cleaved by the addition of iodine.[20-22]

The experimental site-specific cleavage of a protein backbone may be used in two general ways. The first involves mimicking a natural process. For example, introducing Npg into the linker region of a protease-activated receptor would place the receptor under direct experimental control. (Figure 3.2) This system would have the additional advantage of generating a signal upon photolysis, whereas the channels examined to date with Npg show reduced current after irradiation.

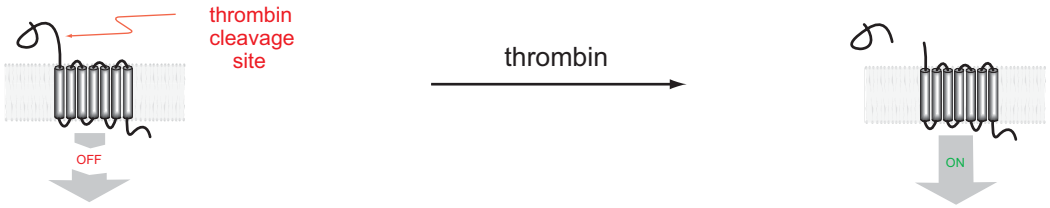

Figure 3.2 Signaling is initiated by proteolysis of the extracellular N-terminal domain of protease-activated receptors.[12]

A second use of *in situ* backbone cleavage is to attempt to map functionally important regions of a protein. This mapping is especially valuable in highly dynamic proteins, such as receptors, where binding of a small molecule induces a conformational change which must be mechanically transduced through the protein. By severing the backbone in a variety of locations, it may be possible to trace the path of conformational changes in the protein. (Figure 3.3)

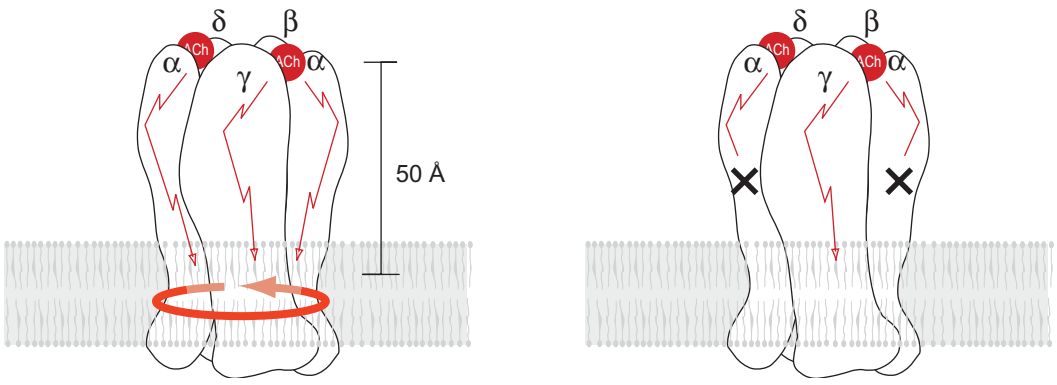

Figure 3.3 Schematic showing how site-specific backbone cleavage may disrupt the pathway of mechanical coupling between binding site conformational change and channel opening.

The ability to target cleavage to a specific residue in a functional protein is obviously of paramount importance to this technique, and this specificity along with the technique's compatibility with living cells represent two of the principal advantages of nonsense suppression.

3.2.2 Previous results with Npg in the nAChR

We have seen in the previous chapter how acetylcholine and nicotine binding may be modulated in the nicotinic acetylcholine receptor. Here, we turn our attention to the biological consequences of agonist binding. The binding of two molecules of agonist to the receptor triggers a conformational change which opens the transmembrane pore of the channel. Relating binding to gating, as this conformational change is called, is fundamental to the process by which a chemical synapse works. The binding of neurotransmitters released by the pre-synaptic cell to ion channels on the post-synaptic cell allows the entry of cations into the post-synaptic cell, thus accomplishing propagation of an action potential from pre- to post-synaptic cell. Understanding, in precise molecule detail, how this conformation change occurs in a protein such as the nAChR could have important consequences, such as the ability to design molecules which affect neurotransmission. However, there are no analytical means available to directly answer such a question. Not only is dynamic crystallography a field in its infancy, but multi-subunit integral membrane proteins such as the nAChR are intrinsically extremely difficult to characterize crystallographically.

Given this experimental context, the ability to introduce unnatural amino acids into functioning nAChR may provide an opportunity for understanding the conformational change associated with gating. In the initial report on Npg, data were shown for

incorporation of this photo-cleavable residue into the Cys loop of the alpha subunit.[1] The Cys loop is a characteristic amino acid sequence which defines the nAChR family of ligand-gated ion channels.[23] (Figure 3.4)

Figure 3.4 Presumed location of Cys loop in the nAChR,[24] based on antibody binding studies and apparent glycosylation of Cys142.

At the time this initial study was undertaken, very little structural information on the positioning of this loop was available. An NMR solution structure of a peptide corresponding to the Cys loop, with and without N-linked glycosylation at Asn142, showed the probable structure of the loop itself.[25] Antibodies which were thought to recognize the Cys loop appeared to bind only after certain maturational processes had taken place, probably dimerization of subunit pairs. However, binding ability was lost in the fully folded receptor, suggesting that the Cys loop was occluded in the pentamer.[26] From these studies, it was surmised that the Cys loop was positioned at inter-subunit interfaces.[24,27] Inter-subunit interfaces were in turn thought to be of critical importance in both making up the agonist binding site, and communicating conformational change from the extracellular binding domain to the transmembrane pore region, some 50 Å away.

Cleavage of the Cys loop in the nAChR alpha subunits had a dramatic effect. Upon photolysis, 90% of the whole-cell current was eliminated. This current reduction was unrecoverable. This experiment appeared to corroborate the prevailing view of the

importance of the Cys loop. An additional experiment in the beta subunit was undertaken to examine the ability of the residue to cleave in a transmembrane domain and also to examine the effects of such cleavage. As with alpha Cys loop cleavage, the effect was expected to be marked. The 9' position of the nAChR is highly conserved, with a leucine residue in all known receptor subunits.[28] It was believed that the Leu residues from all five subunits formed a hydrophobic plug of the pore, which was released during the gating process by subunit movement.[29] In accord with this prediction, photolysis of Npg at the beta9' position led to a 50% decrease in whole-cell current, again in an apparently unrecoverable fashion.

Other than affirming the importance of these two regions to receptor function, it was difficult to know how to interpret the results. Binding studies implied that photolysis of the Cys loop left the receptor able to bind ACh, so the effect appeared to be on gating. However, was it possible to further interpret the result in a mechanistic way? Could the relative amounts of current inactivation be explained? In an attempt to gather more information on these important questions, two lines of experimentation were undertaken.

3.2.3 Experimental design

First, Cys-loop cleavage in all four nAChR subunits was planned. The alpha subunit appears to have a special role in receptor activity. In addition to its stoichiometric double representation, it was thought to largely contain the agonist binding site. Functional receptors may have a variety of subunit compositions and stoichiometries, but alpha subunits are absolutely essential. However, by the time the conformational change associated with binding has been transmitted to the channel pore, each subunit appears to contribute equally. The additive nature of each subunit to the gating process was

established, in part, by previous work from this laboratory involving replacement of the Lue9' residue with unnatural amino acids.[30,31] By analyzing the effects of cleavage in the non-alpha subunits, it was hoped that the results would provide additional information to help delineate the contribution of all five subunits to agonist binding and to help interpret the 90% current reduction observed on alpha Cys-loop photolysis.

Second, attempts were made to extend the analysis of Npg cleavage from electrophysiology to direct biochemical observation of cleavage. The complete scission of a protein should be easily observable by techniques such as gel electrophoresis. However, it was not known whether the small amounts of protein produced by nonsense suppression in oocytes would be detectable. It was hoped, again, that direct confirmation of protein cleavage would assist in the interpretation of results obtained with Npg.

3.2.4 Results

3.2.4.1 Cleavage in non-alpha subunits

The requisite mutations were introduced in the beta, gamma, and delta subunits at the positions homologous to alpha132 and 133, where the initial Npg results were obtained. (Figure 3.5)

α: ^{128}Cys Glu Ile Ile Val Thr His Phe Pro Phe Asp Glu Gln Asn Cys^{142}
β: ^{128}Cys Ser Ile Gln Val Thr Tyr Phe Pro Phe Asp Trp Gln Asn Cys^{142}
γ: ^{128}Cys Ser Ile Ser Val Thr Tyr Phe Pro Phe Asp Trp Gln Asn Cys^{142}
δ: ^{130}Cys Pro Ile Ser Val Thr Tyr Phe Pro Phe Asp Trp Gln Asn Cys^{144}

Figure 3.5 Sequence of the Cys loop in all four subunits of embryonic mouse muscle nAChR.

In these experiments, the expected result was rather difficult to predict. A reasonable presumption would have been that the contribution of different subunits in the extracellular domain would be different. After all, the arrangement of subunits around

the pore calls for different interaction, at the very least, with the important alpha subunits. (Figure 3.4) The gamma subunit, which forms two interfaces with alpha subunits, must have its Cys loop packed against an alpha subunit, if this domain is indeed interfacial. Meanwhile, either the delta or beta subunit must not pack against alpha, because of obvious topological restraints. Upon incorporation of Npg into the receptor, photolysis gave a uniform result. (Figure 3.6)

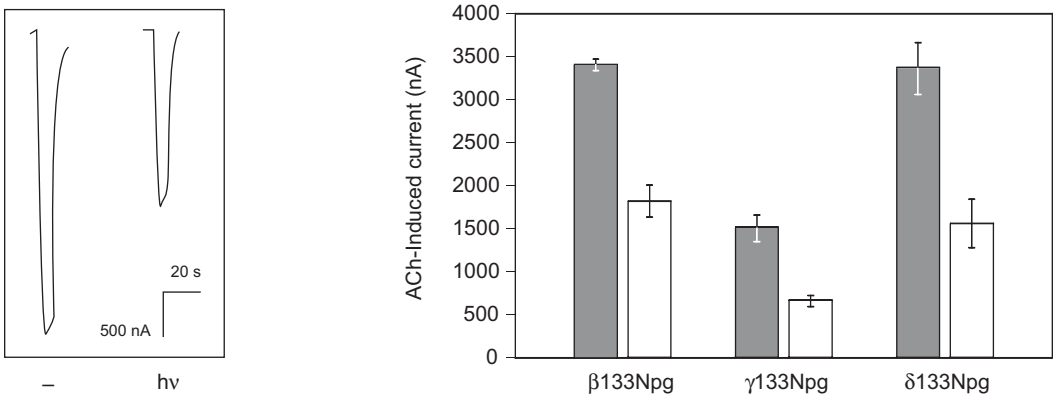

Figure 3.6 Photolysis of nAChR containing Npg in non-alpha Cys loops leads to a consistent 50% reduction in whole-cell current. Left panel: Representative traces from oocytes expressing nAChR with Npg at the γ133 position, without (left) and with (right) photolysis. Right panel: Whole-cell currents from oocytes expressing nAChR suppressed at the indicated position in the presence and absence of irradiation. Filled bars represent mean current (±SEM) in the absence of photolysis. Hollow bars represent mean current (±SEM) from oocytes photolyzed for 4 hr.

In each case, approximately 50% reduction in whole-cell current was observed. The interpretation of this result is by no means straightforward.

One observation which complicates the interpretation of Cys-loop cleavage in non-alpha subunits is the presence of large amounts of background current. Suppression in the alpha subunit of the nAChR typically works very well, with respect to the null control. Co-injection of mRNA and non-aminoacylated tRNA usually produces no observable whole-cell current. In non-alpha subunits, this null control is capable of giving rise to currents of 50% of the maximum suppressed current. (Figure 3.7)

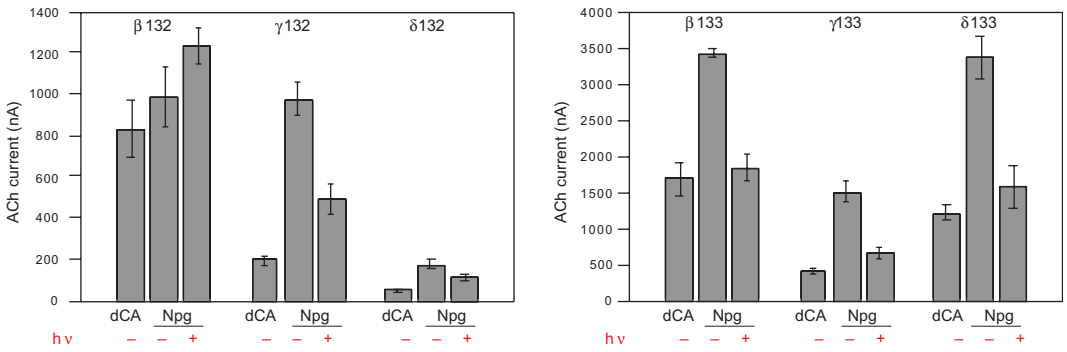

Figure 3.7 Whole-cell currents from oocytes expressing nAChR suppressed with Npg show both the significant background and clear effect of photolysis. Mean currents(±SEM) in response to 200 μM ACh, 24 hr post-injection.

The reason for this difference in behavior is unclear, but there is always concern that receptors with truncated non-alpha subunits or even with non-canonical stoichiometry ($\alpha_2\beta\delta_2$, for example) may be functional.[32] Alternatively, it may be the case that the amounts of read-through (the term is used here to refer to the formation, by any mechanism, of full-length protein which lacks an unnatural amino acid at the desired position) are small, and that the requirement for two alpha subunits means that very little functional protein is formed which has two alphas arising from read-through. In any case, the large currents seen with this control complicate the analysis. Photolysis generally brings the level of whole-cell current down to the level of read-through current. Should photolysis then be scored as 90-100% for all subunits? Or, is it rather the case that the vast majority of functioning receptors on the surface of an oocyte injected with charged tRNA arise from suppression, and that photolysis of non-alpha receptors gives a 50% current decrease? One way to differentiate between these possibilities would be to analyze the products of nonsense suppression with Npg by polyacrylamide gel electrophoresis.

3.2.4.2 Attempts to visualize proteolysis by PAGE

Since electrophoresis separates proteins by mass, photoinduced cleavage should be very evident in PAGE. Since cleavage requires the presence of Npg, it should also be straightforward to distinguish between suppressed protein and full-length protein produced by read-through. Suppressed protein should be cleavable by irradiation, whereas read-through protein will not be. It should be noted that, in the absence of direct evidence for cleavage, there is an additional difficulty in interpreting an experiment with Npg. Has the residue actually cleaved the backbone, or has some conformational change occurred which produces the observed effect? Thus, the ability to directly observe cleavage would simplify analysis by reducing the number of formal possibilities that need to be considered to explain a given result.

The first thing which needs to be established is whether or not protein from suppressed oocytes can be detected by PAGE. The three most common ways of visualizing expressed protein are staining by dyes (Kumasi blue, silver, Ponceau, etc.), detection with antibodies in Western blotting, and by radiolabeling the protein, usually metabolically. These three assays vary in both sensitivity and specificity. Given that oocytes are very large cells with large numbers of membrane proteins, as well as yolk components and vitelline membranes, it was thought that Western blotting might provide an appropriate level of specificity. Sensitivity in a Western blot is largely governed by the affinity of the antibody for its protein target. A number of subunit-specific nAChR antibodies exist which are competent to recognize the denatured protein present in PAGE. However, greater sensitivity may often be gained through the use of epitope tags,

where epitopes for which very high-affinity antibodies exist are introduced into the protein.

Figure 3.8 shows that nAChR from oocytes suppressed with Npg may be detected in Western blotting with anti-nAChRα antibodies. Note also that large amounts of truncated protein are detected in this assay. The domain recognized by Mab 210 is in the extracellular region of the protein, N-terminal to the introduced stop codon.[33] The rather large ratio of truncated to full-length protein illustrates the partial efficiency of the suppression process. In addition, the lack of signal for nAChRα suggests the need for a more sensitive assay.

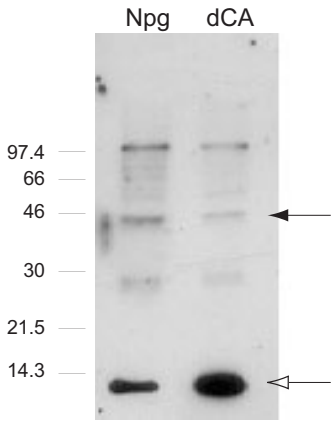

Figure 3.8 Western blot of total membrane preparations from oocytes expressing nAChR suppressed with Npg at position α132, using Mab210 as the primary antibody.[33] Solid arrow indicates full-length alpha subunit. Hollow-headed arrow indicates protein truncated at the 132 position.

Initial attempts to introduce epitope tags into nAChR subunits focused on two widely used tags recognized by the FLAG and HA antibodies. Introduction of an epitope tag potentially constitutes a significant perturbation of the protein's structure. The FLAG epitope is a highly charged sequence of amino acids, optimally DYKDE.[34] The HA sequence is the nine-amino acid YPYDVPDYA.[35,36] In order to determine whether or not introduction of the epitope tag sequence was disruptive to the receptor's function, the

sequences were introduced into a number of regions and the expression of the receptors tested. The FLAG tag had dramatic and negative effects, almost completely eradicating whole-cell nAChR current in all four positions. The HA tag was also highly disruptive at one position in the M3-M4 loop and also at the C-terminus. However, a site with minimal effect on whole-cell current was identified. In addition, it was verified that the HA tag could be introduced at the homologous position in each of the four nAChR subunits. (Figure 3.9) Non-alpha subunits were generally somewhat more tolerant, in that C-terminal HA tags were accepted with little loss of expression. However, for general use the M3-M4 loop position which worked well for alpha was adopted for the other subunits as well. (Figure 3.9) Finally, dose-response relations were found to be unaffected for HA-containing receptors relative to their wild-type counterparts.

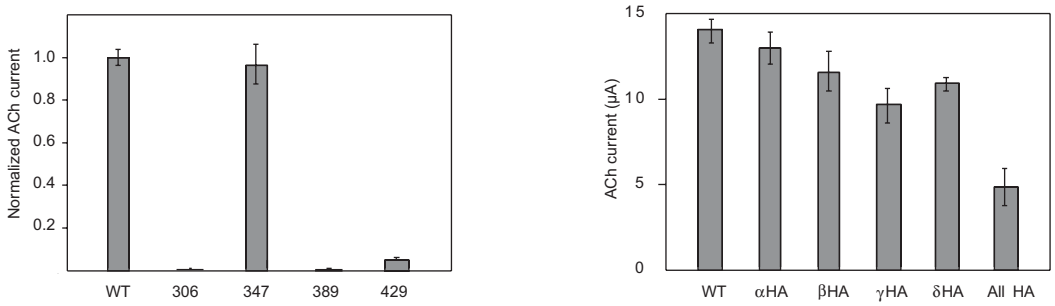

Figure 3.9 Effect of the introduction of the HA epitope tag into nAChR subunits on whole-cell ACh current in response to 200 μM ACh, 24 hr post-injection. Left panel: Mean whole-cell currents (±SEM) resulting from injection of 780 pg mRNA [2:1:1:1] containing an alpha subunit with HA tag inserted at the indicated residue number. Right panel: Mean currents (±SEM) upon injection of nAChR subunit mRNA, where the indicated subunit contains the HA tag at the M3-M4 loop position homologous to α347.

The ability of the epitope tag to render the subunits detectable in Western blots also had to be tested. Isolation of membrane proteins from *Xenopus* oocytes was undertaken in two ways. The first preparation relies on ultracentrifugation of homogenized oocytes, to harvest all of the cell's membranes.[37,38] If sub-cellular fractionation of the various internal membranes is required, this total membrane preparation may be subjected to

sucrose-gradient centrifugation.[39,40] This technique separates the membranes by density, which differs as a result of the varying lipid and protein content of various membrane compartments. Figure 3. shows the results of membrane fractionation. The direct comparison of staining with the anti-HA and Mab210 antibodies shows the superior signal strength of the antibody directed against the epitope tag.

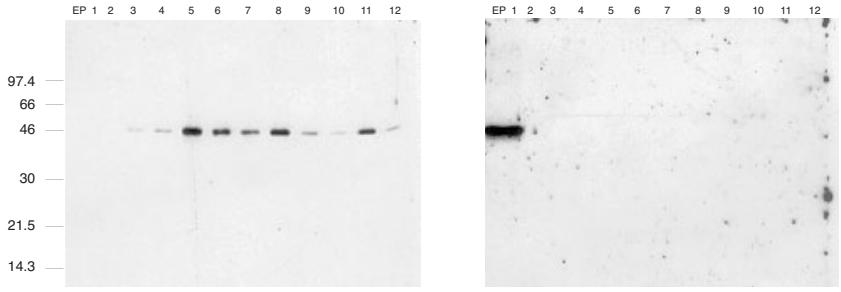

Figure 3.10 Isolation of nAChR from the surface of *Xenopus* oocytes by ultracentrifugation of homogenized oocytes followed by sub-cellular fractionation by sucrose step gradient. Fraction number is indicated above each lane, and molecular weight is indicated to the left. Left panel: Staining with HA.11. Right panel: Staining with Mab210. EP indicates a protein sample from electroplax organs of the *Torpedo* ray (provided by Anthony West).

There are a number of enzyme activity assays which may then be carried out to identify individual membrane fractions. For example, the plasma membrane is the only oocyte membrane to contain a Na^+/K^+ ATPase. Thus, assaying the various fractions for this activity uniquely identifies the plasma membrane.[40] (Figure 3.11)

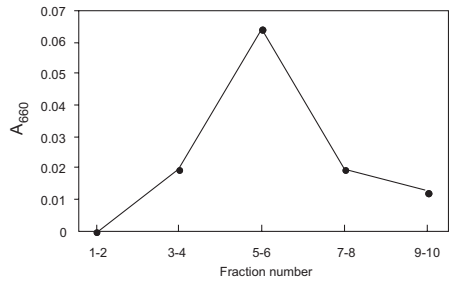

Figure 3.11 Assay for the plasma membrane-resident Na^+/K^+ ATPase, showing that activity is greatest in fractions 5 and 6, which are thus identified as containing the plasma membrane.[40] The assay is based on detection of inorganic phosphate and was carried out by Yan Dang.

A second means of harvesting membrane proteins from oocytes involves physical dissection of the cell.[41] Unlike most cell types, *Xenopus* oocytes have an external glycoprotein membrane known as the vitelline membrane, for its glassy appearance. Unlike a lipid bilayer, this vitelline membrane retains a great degree of structural integrity when isolated from the cell.[42] This rigidity is exploited in a method which fuses the desired plasma membrane with the hardier vitelline membrane. Treatment of the oocytes in a hypotonic solution effects this fusion, as the oocyte swells and the two membranes come in contact.[41] The dissection was found to be facilitated greatly if trace amounts of detergent were present in the hypotonic solution. Figure 3.12 shows membrane proteins isolated from oocytes by physical dissection in the presence and absence of detergents.

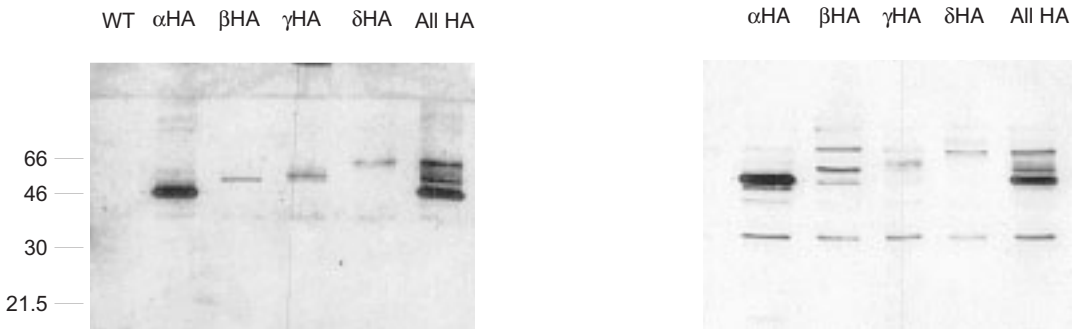

Figure 3.12 Epitope-tagged nAChR subunits isolated from the oocyte membrane and subjected to Western blotting with anti-HA antibody. Subunit which contains the HA tag is indicated above each lane. Note significantly more intense staining of alpha subunits. Left: Fraction 5 from sucrose step gradient subsequent to whole-cell homogenization. Right panel: Protein isolated by physical dissection of oocyte plasma membrane. The non-specific staining in the βHA lane was not typical.

The combination of these techniques to isolate membrane proteins and the use of the HA epitope thus proved satisfactory for visualization of proteins containing unnatural amino acids. It should be noted that staining of non-alpha subunits by the HA.11 antibody is considerably less intense, a phenomenon which is ill-understood but highly

reproducible. Given receptors which may be detected by Western blotting, the analysis of photo-cleavage appeared very straightforward.

Oocytes were irradiated with light of the appropriate wavelength, and whole-cell currents were measured to ascertain whether or not photolysis had occurred. Cells for which current reduction was observed were collected and their membranes harvested for Western blot analysis. In comparison to control oocytes which had not been irradiated, no differences were ever observed. (Figure 3.12)

Figure 3.13 Western blotting of suppressed nAChR βHA L9'TAG and effects of irradiation on Npg-suppressed oocytes. Left panel: Demonstration of suppression at β9'TAG. *Lane 1:* Uninjected. *Lane 2:* mRNA + tRNA-dCA. *Lane 3:* mRNA + tRNA-Val. *Lane 4:* βHA standard. Nine oocytes per lane. Right panel: Effect of irradiation of membrane fraction 3 from oocytes expressing nAChR suppressed with Npg at β9'. *Lane 1:* Irradiated. *Lane 2:* non-irradiated. Four oocytes per lane, whole-cell irradiation for 4 hr at 0 °C.

The explanation for this inability to detect protein fragmentation in response to irradiation remains very unclear. A number of factors complicate the ability to correlate the intensity of bands on the gel to the electrophysiologically observable effect of photolysis.

3.2.4.3 Read-through gives background current and gel bands

It seems evident that there is some read-through of stop codons, as full-length epitope-containing proteins may readily be detected in oocytes co-injected with

uncharged tRNA. The degree to which read-through is observed is rather variable, as may be seen by comparing the relatively light band intensity in Figure 3.13 with the currents observed in oocytes injected with uncharged tRNA in Figure 3.14. Indeed, during the course of these studies, an extremely surprising observation was made. As indicated earlier, the co-injection of mRNA with non-aminoacylated tRNA is a routine null control. These tRNA's are ligated to dCA, so that they are treated in exactly the same way as charged tRNA's. Typically, this 76 nt tRNA-dCA gives much larger currents than mRNA injected alone, but much smaller currents than in cells injected with aminoacylated tRNA carrying a natural or unnatural amino acid. In attempting to identify the source of full-length read-through protein, tRNA which had not been ligated to dCA (i.e. 74 nt tRNA missing the critical CCA motif found at the 3' end of all tRNA) was co-injected with mRNA containing a stop codon. To our great surprise, this 74mer produced larger currents than tRNA-dCA, although still much smaller than those from oocytes injected with charged tRNA. A comparison of a number of tRNA constructs was made. (Figure 3.14)

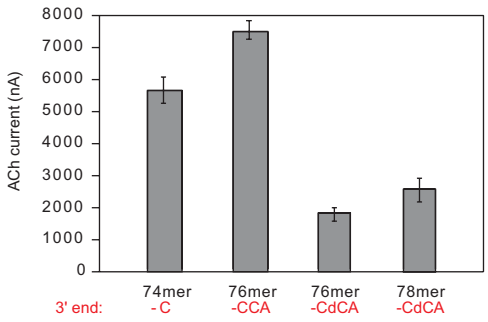

Figure 3.14 Whole-cell currents resulting from the co-injection nAChR mRNA containing β9'TAG with indicated truncated and full-length tRNA.

Eukaryotic tRNA is, in fact, synthesized as a truncated transcript to which the final C, C, and A nucleotides are added by the cytosolic CCA nucleotidyl transferase. The *Xenopus*

isoform has recently been identified.[43] Thus, the 74mer tRNA may well be modified to produce a translationally competent full-length (though uncharged) tRNA. It is presumably this activity which accounts for the ability of the 74mer to produce full-length protein, although it should be noted that no explanation has yet been offered for the exact mechanism of tRNA-mediated read-through.

3.2.4.4 Attempts to eliminate background current by removal of un-ligated 74mer

The fact that 74mer was capable of giving rise to such current led us to the hypothesis that background current in suppression experiments could be eliminated if unreacted 74mer tRNA could be removed after enzymatic ligation of dCA to the 74mer tRNA. The efficiency of this ligation reaction was thought to be on the order of 75%, from the ratio of stained bands corresponding to full-length aminoacylated and 74mer tRNA on sequencing gels. Thus, even when charged tRNA was being injected, a significant amount of 74mer was introduced into the oocyte. Removal of unreacted tRNA was attempted in two ways. First, the vicinal diol of adenine ribose from unreacted dCA was oxidized with periodate. Numerous studies have shown that treating uncharged tRNA with periodate abrogates its ability to function in translation.[44,45] Second, the enzyme polyA polymerase was used in an attempt to add a string of A's to any unreacted tRNA, while charged tRNA would be substitutionally inert.[45,46] It was thought that these polyA tRNA's could then be removed easily using oligo-dT beads, which are traditionally used to capture polyadenylated mRNA from transcriptionally active cells. Neither of these treatments had a significant effect on the electrophysiology of oocytes injected with tRNA subjected to the treatments. One gel showed apparent addition of polyA, although there was little change in the electrophysiology. (Figure 3.) These methods may be

largely irrelevant in light of more recent studies which suggest that the ligation reaction conditions may be modified in such a way as to drive the ligation reaction to completion.[47]

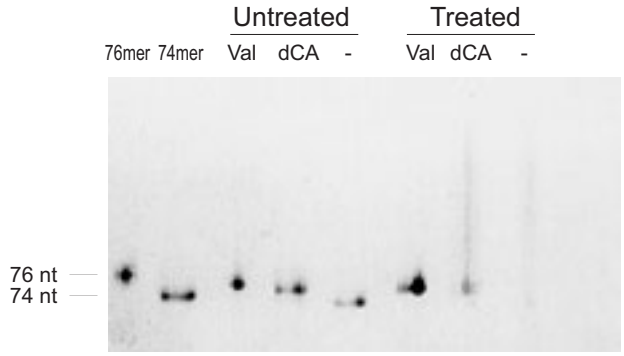

Figure 3.15 SDS-PAGE of ligated and un-ligated tRNA's treated with polyA polymerase subsequent to T4 ligase reaction.

3.2.4.5 Attempts to eliminate background current by tRNA modification

In order for un-ligated tRNA to generate read-through currents, it seems likely that the tRNA must be completed by the nucleotidyl transferase mentioned above. Modifications of the T-loop of tRNA have been reported to compromise the ability of these enzymes to recognize and transfer the final C and A nucleotides to the 3' end of tRNA.[48] TH73G tRNA was accordingly prepared with a G57C mutation. This tRNA was synthetically charged in the usual way by ligation to dCA-Val. Read-through current was indeed dramatically reduced, along with current from suppression. It appears that these mutations may also disrupt ribosome-tRNA interactions, such that the mutant tRNA's are no longer translationally competent.

3.2.4.6 Anomalous subunit trafficking

Another surprising observation which resulted from studies on gel bands resulting from read-through has to do with the fate of nAChR subunits injected alone. The

conventional belief is that single subunits are translated in the ER, but that assembly is required for proper trafficking to the cell surface. Indeed, numerous studies with mammalian cells in culture form the basis for this belief.[49,50] Experiments in oocytes injected with single epitope-tagged subunits suggested that oocytes may be more promiscuous in their trafficking. Harvesting of membranes from such oocytes followed by Western blotting invariably led to detection of the subunits in the membrane fraction. (Figure 3.16)

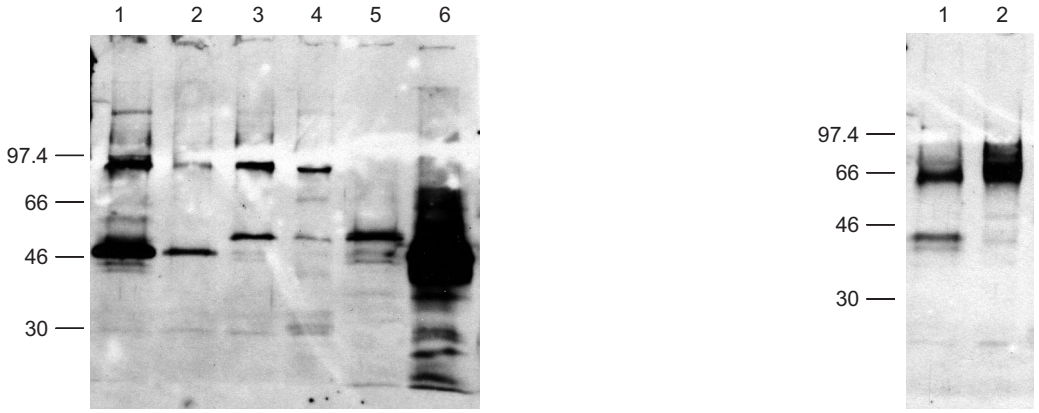

Figure 3.16 Stripped membranes from oocytes expressing HA-tagged subunits either alone or in the full receptor. Left panel: α and β subunits. *Lane 1:* αHA – nAChR. *Lane 2:* αHA only. *Lane 3:* βHA – nAChR. *Lane 4:* βHA only. *Lane 5:* βHA standard. *Lane 6:* αHA standard. Right panel: γ subunit. *Lane 1:* γHA – nAChR. *Lane 2:* γHA only.

It should be noted, of course, that it is extremely difficult to guarantee that a membrane preparation is pure. Interior membranes, scaffolding proteins, and cytoskeletal elements all adhere tightly to the plasma membrane. It is clear during the dissection process that significant amounts of cytosolic tissue are removed along with the fused plasma and vitelline membranes. This difficulty in obtaining pure surface membrane preparations is also a possible confounding variable in attempts to detect photoinduced cleavage of receptors. Although the irradiating light undoubtedly penetrates the oocyte surface to a significant extent (consider the wavelength of 300 nm

light relative to the 3 nm plasma membrane), these sub-surface receptors may not contribute to the observed electrophysiological effects. The apparent cleavage of receptors that is detectable by a loss of whole-cell current may represent only a small fraction of the total receptor protein observed on the gel. Although this does not explain why irradiated sub-surface protein is not photo-cleaved, it does perhaps suggest an explanation for the discrepancy between the electrophysiological result and the result by biochemical analysis.

3.2.4.7 Techniques for harvesting plasma membrane proteins

In an attempt to isolate the surface proteins which were responsible for the measurable electrophysiological change observed upon photolysis, a number of surface-isolation procedures were attempted. The most typical method of this nature is to modify cell-surface proteins with an impermeant reagent, such as an amine-reactive biotin analog. Then, isolation by streptavidin should yield only proteins which were on the surface to be so modified. Indeed, a biotin-based method for detecting oocyte surface expression has been reported.[51] This technique was used apparently successfully, although it gave no better results than manual dissection in terms of visualizing cleavage. (Figure 3.17)

Another surface isolation technique which appeared to be useful was the treatment of the oocytes themselves with antibody, followed by immediate immunoprecipitation.[52] (Figure 3.18) Again, this technique did not allow us to observe fragmentation.

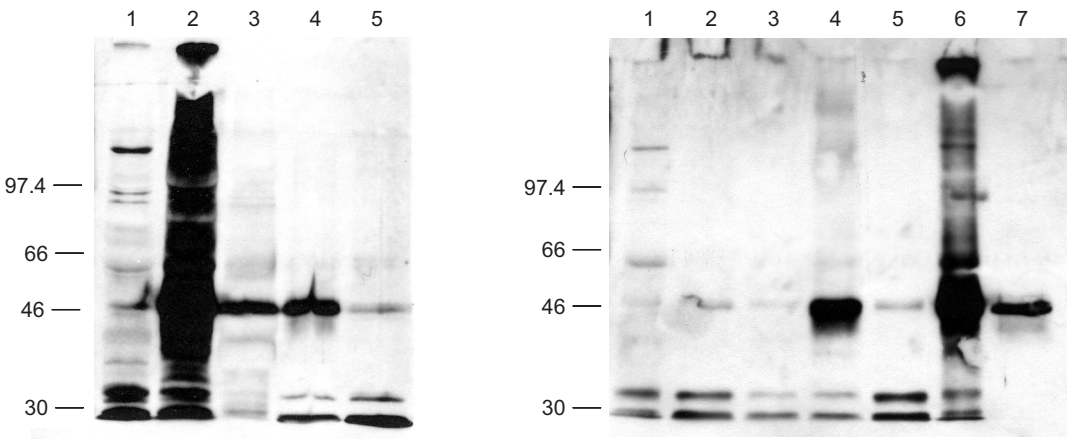

Figure 3.17 Isolation of surface proteins by treatment of oocytes with NHS-biotin followed by streptavidin beads. Left panel: Comparison of whole oocyte, dissected membranes, and streptavidin beads. *Lane 1:* Uninjected – total membranes. *Lane 2:* αHA – total membranes. *Lane 3:* αHA – dissected plasma membrane. *Lane 4:* αHA – streptavidin beads. *Lane 5:* Uninjected – streptavidin beads. Right panel: Capture with streptavidin after surface biotinylation. *Lane 1:* Uninjected – no biotinylation, no beads. *Lane 2:* Uninjected – beads only, no biotinylation. *Lane 3:* Uninjected –biotinylation, beads. *Lane 4:* αHA – biotinylation, beads. *Lane 5:* αHA – beads only, no biotinylation. *Lane 6:* αHA – no biotinylation, no beads. *Lane 7:* αHA standard.

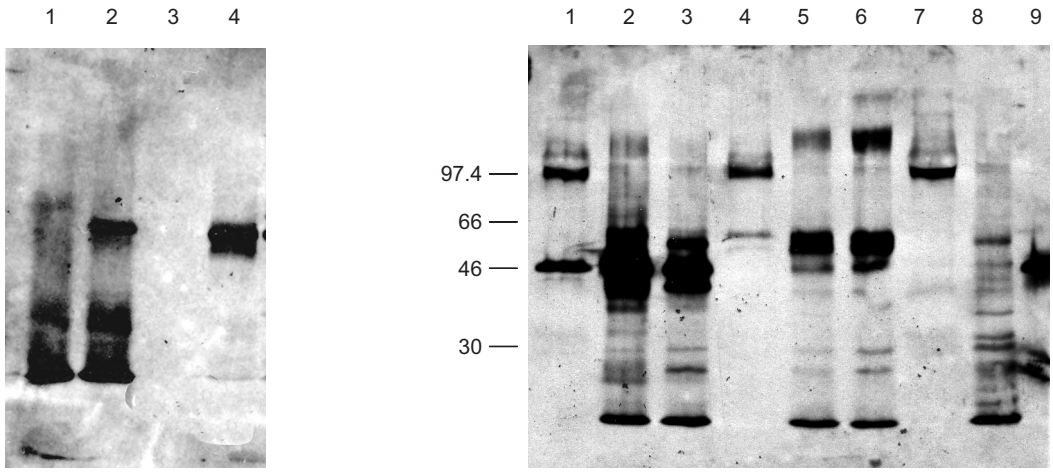

Figure 3.18 Isolation of surface proteins by treatment of whole oocyte with antibodies, followed by recovery with Protein G-sepharose beads. Left panel: Establishing methodology. *Lane 1:* Oocyte homogenate treated with PGS beads. *Lane 2:* Antibody-treated homogenate treated with PGS beads. *Lane 3:* Mab210 and beads only (no oocyte homogenate). Right panel: Testing surface antibody treatment with intra- and extracellular epitope tags. *Lane 1:* αHA – dissected membranes. *Lane 2:* αHA – surface recovery with Mab210. *Lane 3:* αHA – surface recovery with HA.11. *Lane 4:* γ497HA – dissected membranes. *Lane 5:* γ497HA – surface recovery with Mab210. *Lane 6:* γ497HA – surface recovery with HA.11. *Lane 7:* Uninjected – dissected membranes. *Lane 8:* Uninjected – surface recovery with HA.11. *Lane 9:* αHA standard.

3.2.4.8 Use of immunoprecipitation to increase signal strength

Various immunoprecipitation protocols were used and/or developed, for two reasons. First of all, we felt that we could use the techniques to concentrate the protein. Secondly, we were concerned that perhaps the cleaved fragments were being preferentially lost during membrane isolation. Photolysis of Npg-containing proteins captured on beads would allow us to both irradiate a large number of proteins in a very small area and also to analyze beads and supernatant directly after irradiation, to minimize any possibility of protein loss. As with the isolation of cell-surface proteins, we found that we were able to immunoprecipitate suppressed nAChR, but this isolation did not allow us to detect any effect of photolysis. (Figure 3.19)

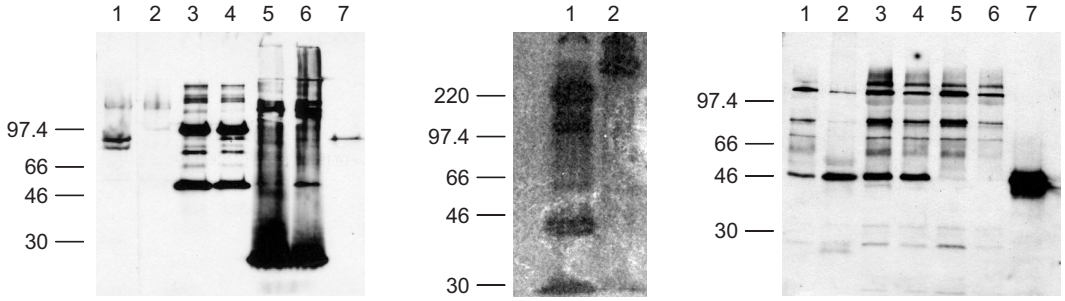

Figure 3.19 Immunoprecipitation protocols. Left panel: Immunoprecipitation from oocyte homogenate with Mab210 and HA.11 affinity matrix, followed by Western blot with HA.11. *Lane 1:* αHA, IP protocol without antibody. *Lane 2:* Uninjected oocytes, IP protocol without antibody. *Lane 3:* Uninjected, Mab210 IP. *Lane 4:* αHA, Mab210 IP. *Lane 5:* Uninjected, IP with HA affinity matrix. *Lane 6:* αHA, IP with HA affinity matrix. *Lane 7:* αHA standard. Protein was eluted from the affinity matrix with HA peptide. Note the very small amounts of recovered αHA relative to antibody. Middle panel: Metabolic labeling with ^{35}S-Met followed by immunoprecipitation with HA.11. *Lane 1:* αHA, IP with HA.11. *Lane 2:* αHA, dissected membranes. Right panel: IP with HA.11 followed by Western with biotinylated HA.11 and streptavidin-HRP. Also, testing the effect of SDS on membrane dissection. *Lane 1:* αβγδHA, dissected membranes. *Lane 2:* αβγδHA, IP with HA.11. *Lane 3:* αHA, dissected membranes (using SDS). *Lane 4:* αHA, dissected membranes (without SDS). *Lane 5:* αHA subunit injected alone, dissected membranes (with SDS). *Lane 6:* αHA subunit injected alone, dissected membranes (without SDS).

3.2.4.9 In vitro photolysis experiments

Ultimately, protein containing Npg was generated from *in vitro* translation and irradiated under non-physiological conditions. The results from oocytes gave us confidence that we could detect suppressed protein by Western blotting. Even if we were unable to recover cleaved protein from oocytes, we felt we should be able to make the protein, irradiate it, and see that it gave rise to two bands on the gel. Even this elementary experiment failed, however. The primary technical difficulty was a general loss of protein upon photolysis. Even recovery of wild-type protein was significantly and adversely affected by photolysis in the arc lamp. Pre-coating of the Eppendorf tubes in which irradiation was taking place failed to ameliorate this problem. Both BSA and coatings such as silicone and polylysine were tested, with negative results. In spite of the reduction of protein levels, it was obvious nonetheless that a band corresponding to cleaved protein was not appearing in the photolyzed samples. It was hypothesized that the alpha-keto acid formed as a photoproduct from the C-terminal cleavage fragment was perhaps susceptible to attack and thus cross-linking by nucleophilic residues on the N-terminal fragment. Photolysis in the presence of nucleophilic scavengers such as semicarbazide was attempted, again with negative results.

3.2.4.10 Cross-linking as a positive control for detecting chemical modification

The final kind of experiment that was attempted was a positive control to demonstrate that some chemical modification of any kind could be observed with suppressed proteins. A brief and unsuccessful attempt was made to treat oocytes with trypsin, to provide evidence that cleaved proteins could be isolated and detected from oocytes. More thorough experiments were performed, using chemical cross-linking as the positive

control for detectable chemical modification. In these experiments, the results of Schmalzing *et al*. on nickel bead-captured 7His-containing nAChR were used as a model.[53,54] Constructs were generated containing the C-terminal 7His tag and the HA epitope in the M3-M4 loop. Subsequent to capture on nickel-NTA agarose beads, protein was treated with DMS, the cross-linking reagent employed by Schmalzing.[53] This experiment gave decidedly mixed results. Higher-molecular weight density was observable in the treated lanes, but under no circumstances were we able to reproduce the discrete bands seen in the reported work.[53] (Figure 3.20)

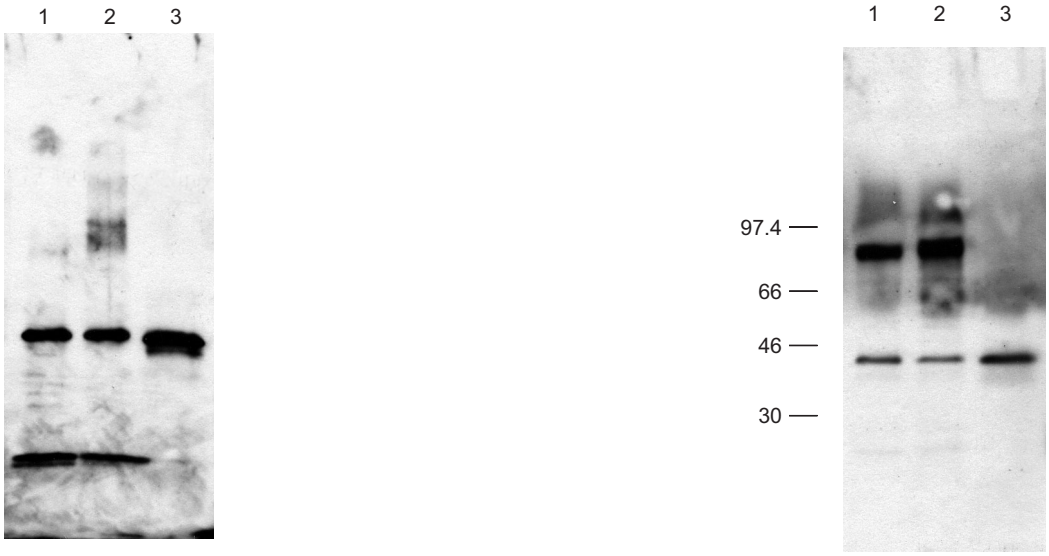

Figure 3.20 Results from treatment of oocytes and nAChR captured on Ni-NTA with the cross-linking reagent DMS. Left panel: Treatment of nAChR captured on beads with DMS, as in the procedure of Schmalzing.[53] *Lane 1:* αHA untreated. *Lane 2:* αHA treated with DMS. *Lane 3:* αHA standard. Right panel: Western blot showing the lack of higher-MW bands from membranes dissected from DMS-treated oocytes. *Lane 1:* αHA untreated. *Lane 2:* αHA treated with DMS. *Lane 3:* αHA standard.

The only substantive difference we could identify between the two experimental protocols was the fact that we were using immunological detection, whereas their protocol called for metabolic labeling with ^{35}S. Oocytes were accordingly labeled, with more or less identical results to our Western blots. Higher molecular-weight density

could be again discerned but not as discrete bands. Another report whose results we were unable to replicate was Hucho's treatment of oocytes with DMS.[55,56] In their experiment, they observed a reduction in whole-cell current upon treatment of oocytes with DMS.[56] In our initial experiments, the treatment had no effect at all, either electrophysiologically or by SDS-PAGE. (Figure 3.20)

A number of different cross-linkers and conditions were used during the course of these experiments. Many of them gave encouraging results, but it was also observed that artifactual aggregation which persisted during standard reducing SDS–PAGE conditions could arise from certain purification steps. (Figure 3.21)

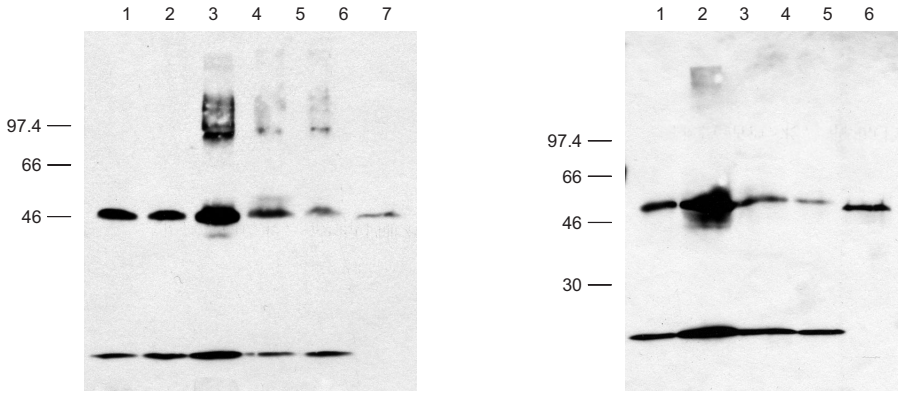

Figure 3.21 Apparent cross-linking is shown to be artifactual by heating gel samples prior to loading. Left panel: Investigation of Ni-NTA recovery protocol and treatment of captured protein with photo-crosslinking reagents. Oocytes were injected with 500 pg total mRNA containing alpha subunits that have both HA and 7His tags. *Lane 1:* Usual Ni-NTA protocol. *Lane 2:* Second imidazole elution from beads in usual protocol. *Lane 3:* Washing and elution of beads using a spin column. *Lane 4:* Treatment of captured protein with DASD. *Lane 5:* Treatment of captured protein with SANPAH in DMSO. *Lane 6:* αHA standard. Right panel: Same samples as left panel, except treated by heating to 100 °C for 10 min.

Collecting and washing Ni-NTA beads by low-speed centrifugation in fritted Eppendorf tubes is a very convenient procedure which results in high yields of protein. However, it appeared to induce aggregation, which could be alleviated by heating samples prior to loading. Apparent cross-linking with covalent reagents was thus also

revealed to be artifactual. As this effort to achieve cross-linking was somewhat peripheral to our interests, it was not pursued further.

3.2.4.11 Ni-NTA purification as a general technique

However, the ability to isolate pentameric nAChR by nickel-mediated capture of receptors containing a C-terminal 7His tag is potentially useful for a variety of biophysical studies. An experiment was performed to determine where receptors isolated from both oocyte homogenate and dissected membranes in the presence of the detergent β-dodecylmaltoside (DDM) maintain their inter-subunit contacts.[13] Oocytes were injected with a mixture of alphaHA and alpha7His subunits. The capture protocol should pull down only those receptors with a 7His tag, whereas the Western blotting detection protocol should only detect those with the HA tag. If the alpha subunit may de detected in a Western blot, the implication is that the two alpha subunits are captured as a non-covalent complex.

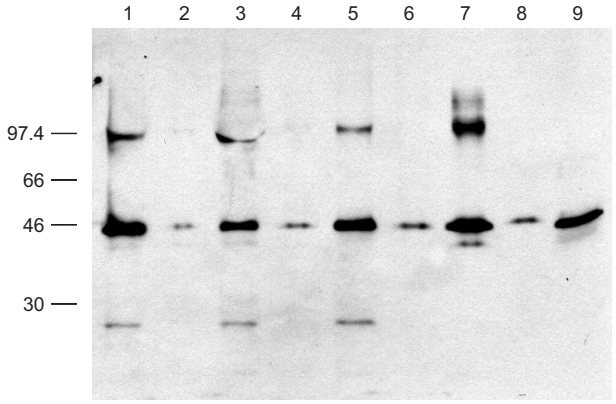

Figure 3.22 Determination whether dissection and Ni-NTA capture protocols with a variety of detergents maintain nAChR in its pentameric form. *Lane 1:* αHA:α7H – dissected membranes, no detergent. *Lane2:* αHA:α7H –Ni-NTA, no detergent. *Lane 3:* αHA:α7H – dissected membranes, with DDM. *Lane 4:* αHA:α7H – N-NTA, with DDM. *Lane 5:* αHA:α7H – dissected membranes, with SDS. *Lane 6:* αHA:α7H – Ni-NTA, with SDS. *Lane 7:* αHA:α7H – oocyte homogenate, Ni-NTA, DDM. *Lane 8:* αHA/7H – positive control, where alpha subunits contain both HA and 7His tags, Ni-NTA, SDS. *Lane 9:* αHA standard.

The results of this experiment imply that the pentamers remain intact in the presence of DDM, consistent with other studies on multi-subunit integral membrane proteins.[13] (Figure 3.22) In our work, SDS also appeared to maintain the intact receptor. The Ni-NTA isolation protocol was performed on dissected membranes, except in one case where it was carried out homogenized oocytes (Lane 7). In all cases, Ni-NTA results in a more pure sample, but one where the signal is correspondingly diminished. The negative control, where non-His tagged subunits are used, generally results in very little background, but there is also frequent variation between batches of oocytes, and such a control in this experiment is probably necessary to support the conclusion that the nAChR remains intact during isolation. However, the results are encouraging. In addition, techniques which only require the labeled subunit to be isolated have been carried out with these constructs in the work of John Leite.[57] Whether or not Ni-NTA purification will provide a means of purifying suppressed receptors remains to be seen.

3.2.5 Conclusions from non-alpha Npg cleavage

In summary, cleavage of proteins containing Npg was never able to be directly observed by PAGE. However, the whole-cell current of oocytes expressing nAChR with Npg in non-alpha Cys loops was reproducibly reduced to the level of dCA current. In the absence of biochemical evidence on cleavage, we were unable to determine whether this effect corresponds to 90% cleavage of Npg-containing receptors, with nAChR arising from read-through accounting for the residual current; or 50% cleavage of Npg-receptors, with un-cleaved receptors accounting for the remainder of the current.

One experiment which may shed light on this question was the determination of the dose-response pre- and post-photolysis. A change in the EC_{50} of the receptor may imply

that receptors have been affected by photolysis, as we had already shown that the read-through currents had the same EC_{50} as wild-type receptors. In fact, the EC_{50} values of receptors containing Npg in non-alpha Cys loops is identical before and after photolysis, even in cells where a 50% reduction in whole-cell current was observed. (Figure 3.23)

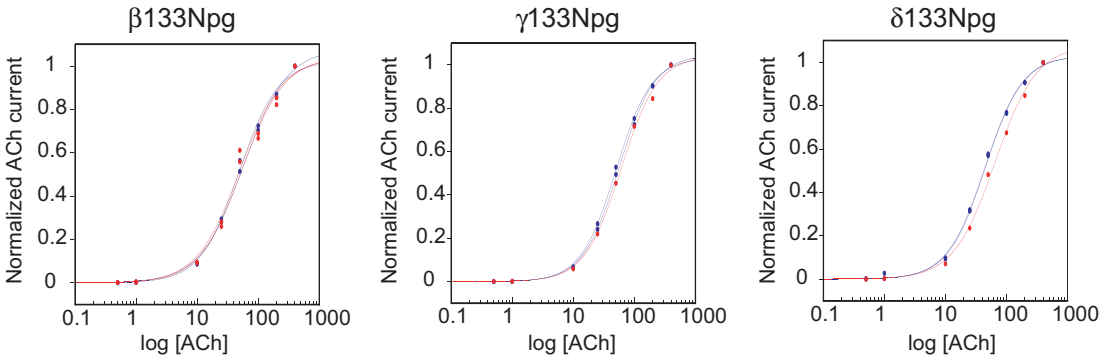

Figure 3.23 Dose-response relations for oocytes expressing nAChR suppressed with Npg in the indicated position, fit to the Hill equation. Photolyzed oocytes are indicated in red and un-photolyzed cells by blue.

Thus, interpretation of the results obtained by the photolysis of receptors containing Npg in non-alpha Cys loops remains difficult. A number of useful biochemical techniques were developed during the course of the study, including the use of epitope tags, methods for isolation of suppressed receptors from oocytes, detection of suppressed receptors in Western blots, immunoprecipitation in oocytes, *in vitro* translation of suppressed proteins using wheat germ extract, cell-surface labeling of oocytes, and purification of suppressed proteins by Ni-NTA.

3.3 Site-specific photocrosslinking with Bpa

3.3.1 Introduction to site-specific crosslinking

Both the difficulties in structurally characterizing membrane proteins and the large number of stoichiometries available to neuroreceptors have been mentioned above. In

addition, a great deal of active research is directed toward understanding the modulation of ion channel activity by protein-protein interactions, the targeting of ion channels to the cell surface by cytoskeletal interactions, and the localization of channels to membrane rafts and the proteins associated with them.[58-60] A general technique to identify the interaction partners of ion channel subunits would be of great utility. In addition, the ability to identify regions of a particular protein or subunit which constitute an interaction domain or protein-protein interface would be valuable for relating the primary sequence of a protein to the structure-function relationships inherent in its domain organization.

A number of photoactive functional groups have been employed in the design of photo-crosslinking reagents. The most common types, aryl azides, diazirines, and benzophenone-based molecules have been reviewed.[61] The various chemistries have advantages and disadvantages and are appropriate for different contexts. Experiments using diazirines introduced by nonsense suppression played an important part in establishing the role of the translocon in membrane protein synthesis.[62,63] However, some work performed here and elsewhere suggested that benzophenone-based residues may incorporate more efficiently under the conditions used in our laboratory.[2,64] In collaboration with Justin Gallivan, who had previously prepared dCA-Bpa, the work described here was carried out using 4-benzoylphenylalanine (Bpa).[64] (Figure 3.24)

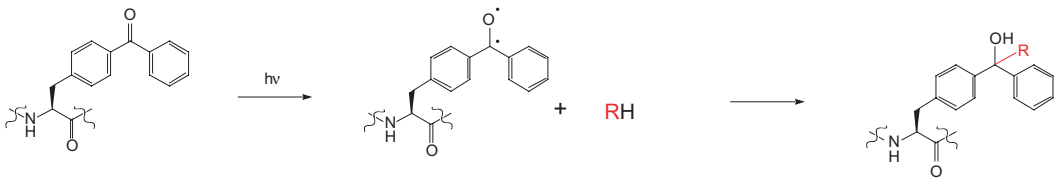

Figure 3.24 Schematic of the cross-linking chemistry of benzoylphenylalanine (Bpa). Irradiation of the residue leads to a biradical, which abstracts hydrogen from a neighboring side chain. The resulting covalent linkage may be an intrasubunit crosslink, or if the residue is interfacial, an intersubunit linkage.

Suppression was attempted with the photoactive residue in every position in the Cys loop of the gamma subunit of the nAChR. As indicated earlier, the belief at that time was that the Cys loop constituted a portion of the intersubunit interface. The position of gamma between the two alpha subunits was seen as desirable, in that cross-linking to alpha seemed probable. In addition to the fact that the stoichiometry of the receptor makes labeling both alpha subunits with the HA epitope tag trivially easy, it is also the case that the sensitivity of alphaHA in Western blots is higher than that of other subunits.

After introduction of the Bpa residue, the oocytes were tested for expression in the standard two-electrode voltage clamp configuration. Suppression was achieved at a number of sites, although several never gave appreciable current over background levels. (Figure 3.25) Additional data on the suppression efficiency is available.[64]

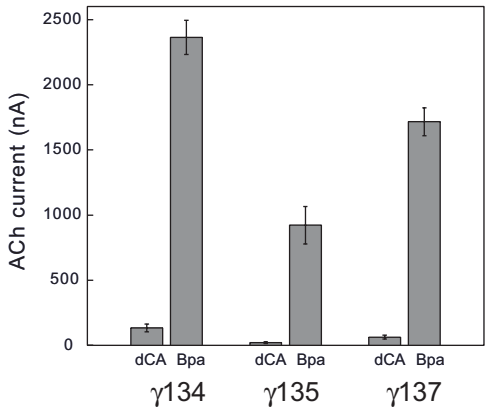

Figure 3.25 Suppression of Bpa at selected sites which gave good expression in the nAChR gamma Cys loop. Mean whole-cell currents (±SEM) are indicated.

Oocytes giving measurable whole-cell currents were then photolyzed in batches for four hours, using the same conditions as employed for Npg cleavage. After photolysis, the oocytes were recorded from. In addition, the membranes were dissected away and analyzed for high-molecular weight products arising from cross-linking between the alpha and gamma subunits. Both of these studies were in all cases negative. No

electrophysiological effects were ever observed to arise from photolysis. Nor were higher-molecular weight bands ever observed in Western blotting. (Figure 3.26)

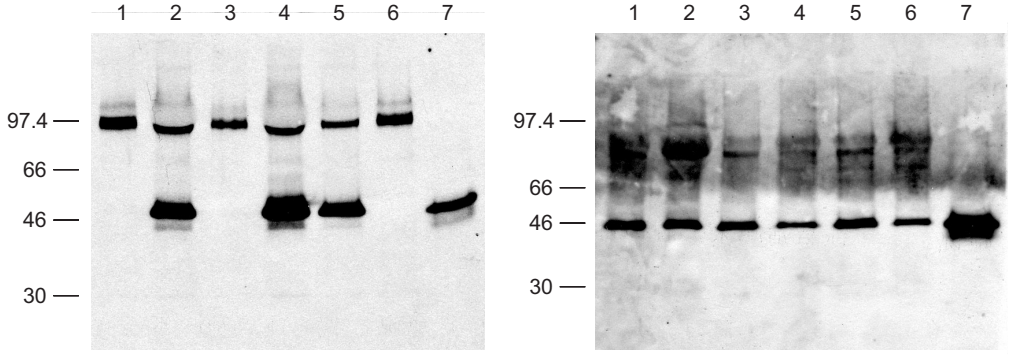

Figure 3.26 Western blotting from irradiated oocytes containing Bpa at a variety of sites in the gamma Cys loop, showing the lack of detectable cross-linking. Left panel: Irradiation of oocytes containing nAChR γ129Bpa followed by dissection of plasma membranes. *Lane 1:* Uninjected oocytes. *Lane 2:* γ129 Bpa. *Lane 3:* Uninjected, photolyzed 4 hr. *Lane 4:* γ129 Bpa, photolyzed 4 hr. *Lane 5:* γ129 Bpa, photolyzed in arc lamp. *Lane 6:* Uninjected, photolyzed in arc lamp. *Lane 7:* αHA standard. Right panel: Irradiation of oocytes containing nAChR γ134-137Bpa followed by dissection of plasma membranes. *Lane 1:* γ134 Bpa. *Lane 2:* γ134 Bpa, 4 hr hν. *Lane 3:* γ135 Bpa. *Lane 4:* γ135 Bpa, 4 hr hν. *Lane 5:* γ137 Bpa. *Lane 6:* γ137 Bpa, 4 hr hν. *Lane 7:* αHA standard.

Thus, although site-specific cross-linking remains an attractive use of unnatural amino acid mutagenesis, Bpa incorporation in the Cys loop of gamma appears in hindsight to have had little chance of success. The crystal structure of AChBP shows the Cys loop to be rather ill-positioned for intersubunit crosslinking.[65] (Figure 3.27) However, the sequence of this loop is very different from the highly conserved Cys loop sequence found in the family of ligand-gated ion channels, so it is possible that the AChBP is not a reliable indicator of the position of the Cys loop in the full receptor.

Figure 3.27 Two views of the AChBP crystal structure, showing the location of the Cys loop, in red.[65] Left panel: View from what would be the intracellular side of the receptor, if the AChBP contained transmembrane domains. Right panel: View from the side of the protein, where the Cys loops would contact the membrane in a true receptor. One subunit is rendered in dark gray to emphasize the subunit interface.

It may be the case also that the project suffers from a fundamental difficulty, namely, that introducing unnatural amino acids into interfacial regions of proteins is intrinsically destabilizing. This problem could potentially be surmounted by making a longer linker between the peptide backbone and photoactive functional groups in the side chain. Alternatively, serial incorporation of the unnatural amino acid into a contiguous sequence may be able to identify those sites where substitution of the natural side chain for the large hydrophobic Bpa residue is tolerated. Now that a crystal structure exists for the highly homologous AChBP, it may be possible to rapidly determine whether or not inter-subunit cross-linking may be realized with Bpa. In addition, the advent of mass spectrometry from ion channels expressed in oocytes raises the possibility that a more sensitive assay than Western blots may be employed.[57] Success of these proof-of-principle experiments could then justify a more intensive attempt to identify interfacial regions in less well-characterized channels using site-specific photocrosslinking. Thus, the efforts reported here should only be considered as the pioneering stage of a the project and were carried out using what may prove to be highly inaccurate structural assumptions.

3.4 Using hydroxy acids to determine Cys-Cys connectivity of the $P2X_2$ receptor

3.4.1 Experimental design

The unnatural amino acid Npg allows the protein backbone to be site-specifically cleaved in a functioning protein. Compared to this, it may appear that the ability to site-specifically cleave a polypeptide subsequent to isolation of the protein is a rather paltry achievement. However, site-specific cleavage of isolated proteins is a useful technique for solving a particular topological problem. The three-dimensional connectivity of a protein backbone is complicated by the existence of side chain-mediated contacts, namely the disulfide bonds between cysteines. In the absence of three-dimensional structural data, there is no way of knowing which cysteine in a primary sequence may be bonded to another. However, a technique developed by Pam England in this laboratory provides a means whereby site-specific cleavage may be used to determine this connecticity.[4] In this methodology, incorporation of hydroxy acids is used to introduce a specific site between selected cysteine residues where the backbone is base-labile.[3,4] (Figure 3.28)

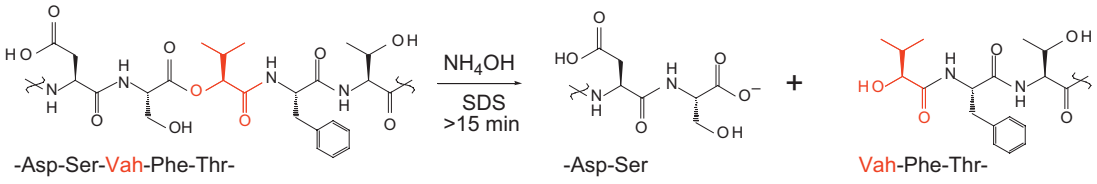

Figure 3.28 Schematic showing how introduction of a hydroxy acid (red) into the protein backbone creates a base-labile linkage.

In general, when a cleavable residue is placed between two disulfides and the protein is cleaved, two outcomes are possible. If the cysteines do not form a disulfide, the protein will be cut in two. If the side chains are connected by a disulfide bond, however, the backbone will be cleaved but the two halves of the protein will remain attached by the

covalent bond between side chains. This difference is easily observable by PAGE. Additional information may be obtained by treatment with reducing agents during electrophoresis. If disulfide-reducing agents are present, the disulfide-bonded halves will separate into two fragments, confirming that backbone cleavage has occurred. (Figure 3.29)

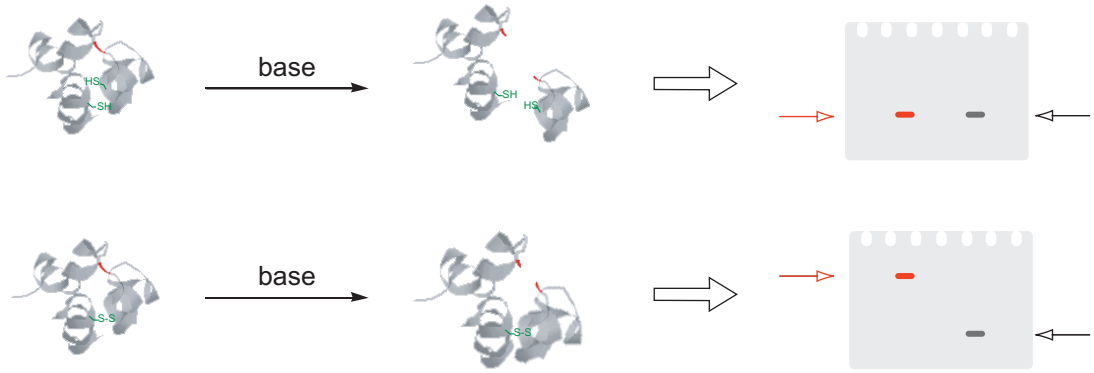

Figure 3.29 Schematic showing how site-specific backbone cleavage may be used to determine the disulfide connectivity of a protein.[4] Targeted inter-cysteine backbone cleavage is followed by comparison of SDS-PAGE mobility in the presence and absence of disulfide reducing agents . The gel mobility of the cleaved protein reveals whether or not the cysteines on either side of the cleavage site are in a disulfide. Red arrows indicate treatment with both base and reducing agent. Black arrows indicate treatment with base alone in the absence of reducing agent.

It has been relatively recently appreciated that disulfides provide small proteins the opportunity to create highly stable scaffolds. A number of disulfide knot toxins have recently been discovered, such as the snail-derived conotoxins.[66,67] These small peptides are able to form a relatively rigid binding domain with excellent complementarity to the extracellular domains of ion channels. The paralytic ability of conotoxins arises because of this binding, which inhibits the nicotinic receptors that motoneurons rely upon to turn synaptic signals into muscle movement. However, toxins are not the only proteins to rely upon disulfides to scaffold binding domains. The primary structure of P2X channels has

recently been determined and has shown these receptors to be extremely cysteine-rich.[68] (Figure 3.30)

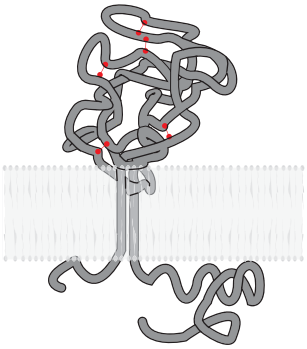

MVRRLARGCWSAFWDYETPKVIVVRNRRLGFVHRMVQLLILLY
FVWYVFIVQKSYQDSETGPESSIITKVKGITMSEDKVWDVEEY
VKPPEGGSVVSIITRIEVTPSQTLGTCPESMRVHSSTCHSDDD
CIAGQLDMQGNGIRTGHCVPYYHGDSKTCEVSAWCPVEDGTSD
NHFLGKMAPNFTILIKNSIHYPKFKFSKGNIASQKSDYLKHCT
FDQDSDPYCPIFRLGFIVEKAGENFTELAHKGGVIGVIINWNC
DLDLSESECNPKYSFRRLDPKYDPASSGYNFRFAKYYKINGTT
TTRTLIKAYGIRIDVIVHGQAGKFSLIPTIINLATALTSIGVG
SFLCDWILLTFMNKNKLYSHKKFDKVRTPKHPSSRWPVTLALV
LGQIPPPPSHYSQDQPPSPPSGEGPTLGEGAELPLAVQSPRPC
SISALTEQVVDTLGQHMGQRPPVPEPSQQDSTSTDPKGLAQL

Figure 3.30 Presumed structure and primary sequence of the ATP-binding receptor $P2X_2$. Extracellular cysteine residues are boxed in red. Sites of stop codon introduction discussed below are indicated with red text.

The predicted 283 aa ATP-binding extracellular region of these channels contains ten cysteine residues. Interestingly, the ATP-binding domain of the P2X receptors has no apparent sequence homology to known ATP-binding folds such as the Walker or Rossman motif.[69-71] So, structural information on the connectivity of the cysteines in the extracellular region of the $P2X_2$ receptor may be a valuable in guide in designing experiments to try to identify where ATP binds.

These experiments were carried out in collaboration with Baljit Khakh, who provided the initial $P2X_2$ constructs. A FLAG epitope was introduced into the receptor at the extreme C-terminus. In these two-transmembrane domain receptors, both termini are intracellular. In addition, he introduced stop codons between all ten cysteine residues. The sites of mutation were chosen based on rules established in the work of England *et al*. for optimal cleavage of hydroxy acids.[3,4] She found that there were sequence context effects on the efficiency of hydrolytic cleavage of hydroxy acids introduced into proteins. The sites chosen in the $P2X_2$ receptor were selected for favorable cleavage. Based on the

work of England, hydroxy acids of valine and alanine were employed for suppression experiments.

Protein isolated from oocytes subsequent to electrophysiological recording was thought to have the best chance of reflecting the native structure of the receptor, an important consideration for an *ex vivo* structural technique. However, it had also been found in the earlier studies of England that protein produced by *in vitro* translation could be valuable for establishing cleavage conditions.[3,4] Whether or not the receptor is being folded correctly in wheat germ extracts may even be determined by comparison to its cleavage behavior relative to that of isolated functional protein.

3.4.2 Results

Initial work in this receptor indicated that the specificity of the FLAG epitope in Western blotting was dramatically inferior to that of the HA antibody. In addition, the overall level expression of the channel was rather low in suppression experiments with hydroxy acids. In order to correct both of these problems, the $P2X_2$ gene was cloned into pAMV and an HA tag inserted at the extreme C-terminus. These changes resulted in increased expression and much better staining in Western blots. (Figure 3.31)

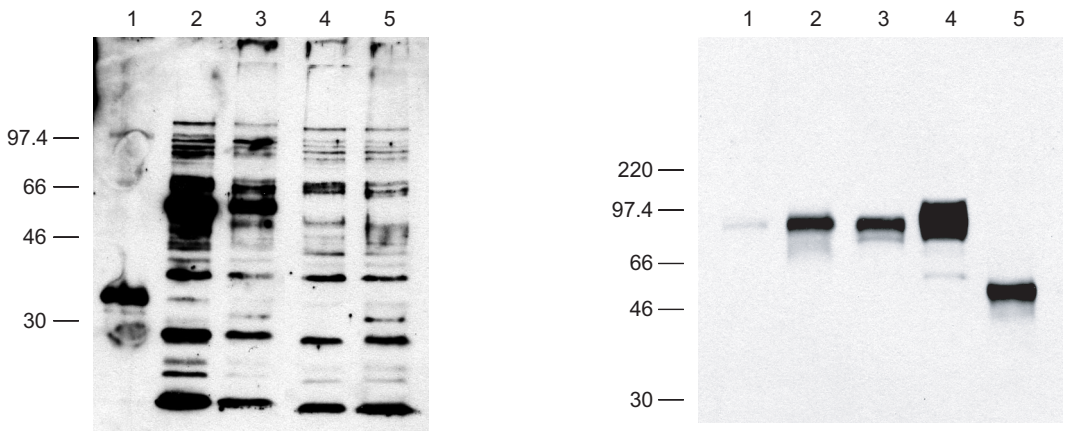

Figure 3.31 Western blot analysis of $P2X_2$ receptors showing the relative efficacy of C-terminal FLAG and HA epitope tags. Additionally, effects of PNGaseF on the receptor are examined, along with potential dominant-negative effects from truncated $P2X_2$ 142TAG. Left panel: Western blot of C-terminally FLAG-tagged $P2X_2$. *Lane 1:* Uninjected, dissected membranes. *Lane 2:* $P2X_2$, wheat germ extract. *Lane 3:* $P2X_2$, wheat germ extract, treated with PNGaseF. *Lane 4:* nAChR αHA/FLAG, wheat germ extract. *Lane 5:* nAChR αHA/FLAG, wheat germ extract, treated with PNGaseF. Right panel: Dissected membranes from oocytes expressing Vah-suppressed $P2X_2$ V142TAG with C-terminal HA tag. *Lane 1:* $P2X_2$ 142TAG, 74mer. *Lane 2:* $P2X_2$ 142TAG, Vah. *Lane 3:* $P2X_2$ 142TAG, mixed with WT $P2X_2$. *Lane 4:* $P2X_2$ wild-type receptor with C-terminal HA. *Lane 5:* αHA standard.

However, two rather knotty problems arose. First of all, wild-type $P2X_2$-HA showed a rather significant mobility shift upon treatment with ammonium hydroxide. (Figure 3.32) This may arise as a result of base-catalyzed hydrolysis of sugars post-translationally added to the receptor. Treatment of isolated wild-type $P2X_2$ with PNGase F, an enzyme which removes *N*-linked glycosylation showed little effect, though, so it may be that *O*-linked sugars or some other base-catalyzed chemistry was responsible for this mobility shift. (Figure 3.31)

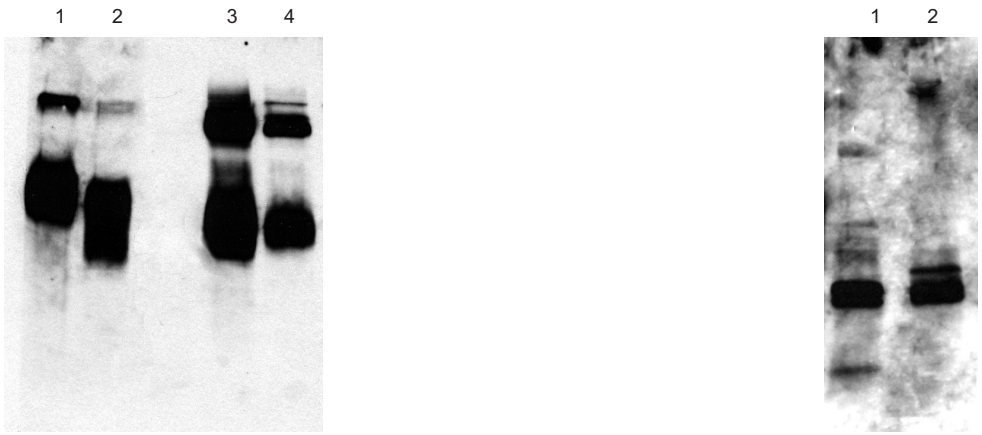

Figure 3.32 Western blot of base-treated $P2X_2$ containing Vah and wild-type residues, and nAChR positive control for ester cleavage. Left panel: Effects of treating Vah-suppressed and wild-type $P2X_2$ with base. *Lane 1:* WT $P2X_2$, treated with NH_4OH and β-ME. *Lane 2:* $P2X_2$ 142Vah, treated with NH_4OH and β-ME. *Lane 3:* WT $P2X_2$, treated with NH_4OH but not β-ME. *Lane 4:* $P2X_2$ 142Vah, treated with NH_4OH but not β-ME. Right panel: Positive control for NH_4OH cleavage and identification of disulfide formation with β-ME, showing cleavage only in the presence of disulfide reducing agent. *Lane 1:* nAChR α131Ser132Vah, treated with NH_4OH and β-ME. *Lane 2:* nAChR α131Ser132Vah, treated with NH_4OH but not with β-ME.

Secondly, incorporation of hydroxy acids worked at very few of the eight inter-Cys positions. (Figure 3.33) This was a surprising result in view of the fact that the amide-to-ester mutation is a rather slight perturbation, that it seemed unlikely that so many of the sites chosen would have represented critical residues to protein function, and that the work of England suggested rather great tolerance to hydroxy acids in the nAChR.[3,4]

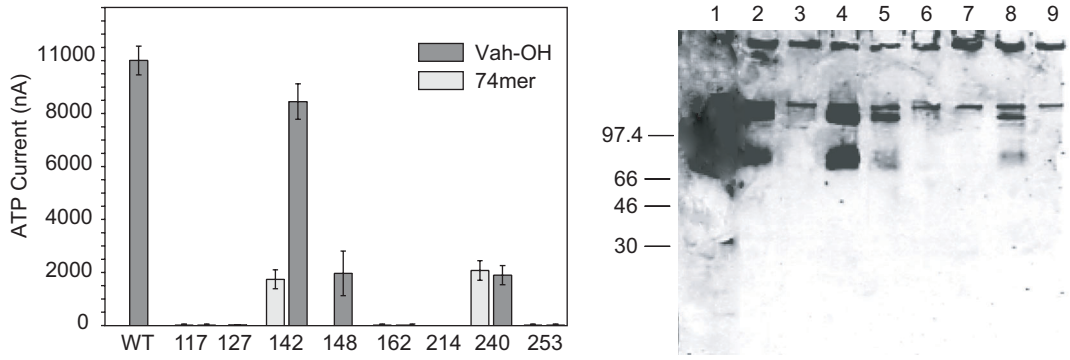

Figure 3.33 Electrophysiological and Western blot analysis showing the relatively low tolerance of $P2X_2$ receptor to incorporation of Vah. Left: Mean whole-cell current (±SEM) for oocytes suppressed with Vah at the indicated inter-Cys position. Right: Western blot of membranes dissected from the Vah-suppressed oocytes shown in left panel. *Lane 1:* WT. *Lane 2:* 117Vah. *Lane 3:* 127Vah. *Lane 4:* 142Vah. *Lane 5:* 148Vah. *Lane 6:* 162Vah. *Lane 7:* 117Vah. *Lane 8:* 240Vah. *Lane 9:* 253Vah.

When compared directly to the wild-type residue, receptors arising from suppression at 142 had somewhat different PAGE mobility. (Figure 3.32) Although the sequencing data from these constructs suggested that the region around the introduced mutation was consistent with the expected sequence, the constructs may well have been faulty. Even if this were the case, however, electrophysiology and Western results confirm that significantly greater current and staining intensity were observed upon supplying the cells with hydroxy acid-charged tRNA. Thus, by all standards currently employed, the hydroxy acid was present in these receptors. In no case was base-induced cleavage observed, however, although altered gel mobility in the presence of base was seen for 142 as well as the wild-type construct. Given the apparent lack of cleavage, a position which gave good cleavage in the nAChR in the earlier work of England was selected for use as a positive control.[3,4] Indeed, cleavage was observed as anticipated. (Figure 3.32)

3.4.3 Future directions

Because of the intractability of the $P2X_2$ system, with both gel mobility of wild-type protein induced by base treatment and no evidence of cleavage in hydroxy acid-containing protein, this line of experimentation was abandoned. Suggestions for the future involve treatment of the receptor with the glycosidase EndoH, which removes both *N*- and *O*-linked sugars, to attempt to resolve the mobility of WT receptor upon base and β-mercaptoethanol treatment. Additional sites of mutation could also be chosen, to determine whether better suppression efficiency might be achievable elsewhere in the receptor.

3.5 Use of photo-labile side chains to induce dynamic conformational change

3.5.1 Experimental design

In the case of Bpa, a photoactive side chain was incorporated for the purposes of cross-linking. Side chains with photo-cleavable protecting groups may also be introduced for the purposes of providing steric bulk which may then be removed by irradiation.[72,73] In this way, a conformational change may be induced experimentally. Typically, this conformational change is rather small, and a sensitive region of the protein is the best site for use of protected side chains for this purpose. Such a region is the gate of an ion channel. As indicated above, a conformational change resulting from binding of a ligand-gated ion channel's agonist is communicated to the gate in the transmembrane regions, resulting in channel opening. In the nAChR, this gate is thought to be near the L9' position.[28,29,31]

In work conducted in collaboration with Ken Philipson, tyrosine and cysteine with the alcohol and thiol, respectively, protected by a nitrobenzyl group, were introduced at the 9' position.[6] (Figure 3.34)

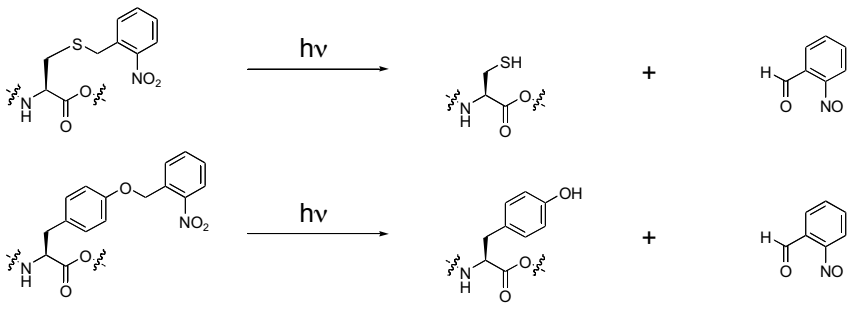

Figure 3.34 Schematic showing photolytic de-caging of Cys(ONb) and Tyr(ONb).

In these experiments, the removal of the protecting group was examined as a possible means of very rapidly controlling channel gating and gaining insight into the temporal mechanics of the gating process.

3.5.2 Results

Suppression in the alpha subunit proved rather inefficient, although better results were obtained in both beta and gamma subunits. Gamma suppression is exclusively considered below. The first observation from application of this technique was that very striking effects of photolysis were immediately evident. (Figure 3.35)

Figure 3.35 Light-induced decaging of Cys and Tyr analogs in the transmembrane region of nAChR γ. Left panel: Light-induced decaging of Cys(ONb). Current was first activated by the application of ACh (20 mM) to an oocyte expressing the ACh receptor. The oocyte had been injected with cRNA coding for wild-type α, β, and δ subunits and for the γ subunit with a Leu260TAG (γ9'TAG) mutation. Suppressor tRNA charged with Cys(ONb) was co-injected. Methanethiosulfonate ethylammonium (MTSEA; 0.35 mM) was included in the bathing medium as indicated. Three pulses of ultraviolet light of 3 s duration each are indicated by arrows. Spikes in current traces are artifacts due to switching of the bathing medium. Right panel: De-caging of Tyr(ONb). Current was activated by the application of ACh (20 μM) to oocytes expressing the ACh receptor. A Leu260TAG mutation was present in the γ-subunit (γ9' position of M2). The stop codon was suppressed by the co-injection of suppressor tRNA charged with Tyr(ONb). Two pulses of UV light of 3 s duration each are indicated by arrows. The current transient induced by the second flash is artifactual, as similar transients were sometimes also seen with the wild-type channel.

With both tyrosine and cysteine, irradiation caused an immediate increase in current. Continued 1 ms pulses of light reveal more and more current, with each flash activating approximately 5% of the available receptors. Detailed kinetic analysis showed that the response to cysteine de-caging was more rapid than could be measured by the apparatus

used. Receptor response to tyrosine de-caging was rather slower, an effect perhaps explained by greater steric perturbation resulting from the larger nitrobenzyl tyrosine residue. Apparently, conformational rearrangement must occur before the channel can respond properly to ligand binding. An alternative explanation might be that the photochemistry is slower for nitrobenzyl tyrosine than nitrobenzyl cysteine, although the efficiency of tyrosine photolysis appears greater than for cysteine.

An additional effect which was observed with tyrosine was that the presence of this residue at the 9'position appeared to greatly enhance ACh open-channel block. A cation-π effect was considered to explain this effect, with the residue being replaced sequentially by Trp and F_4-Trp. In both cases, robust channel block was observed. Substitution of the tyrosine with 4-methyl-tyrosine appeared to abrogate block, however, suggesting that the tyrosyl hydroxyl may have an important role in this effect.

3.5.3 Future directions

The applicability of caged amino acids to transmembrane domains was demonstrated. In order to know whether high-resolution kinetic information could be obtained with these residues, it will probably be necessary to employ rapid electrophysiological techniques, such as single-channel recording. If nonsense suppression is able to be achieved in mammalian cells, it is conceivable that that this technique might be used in situations where ultra-fast control over ion channels is required. Signaling processes associated with conductance could be examined in this way, for example.

As will be seen in the following chapter, caged amino acid side chains may also be used to control certain post-translational modifications. Tyrosine will be considered in depth in this regard in Chapter 4. Numerous processes rely on the modification of

cysteine side chains, such as protein lipidation, and they may be able to be subjected to control by caged cysteine. Thus, the demonstration that this residue is compatible with nonsense suppression is in itself an important precursor to such experiments.

3.6 References

1. England, P. M., Lester, H. A., Davidson, N. and Dougherty, D. A. Site-specific, photochemical proteolysis applied to ion channels *in vivo*. *PNAS* **94**, 11025-11030 (1997).
2. Kanamori, T., Nishikawa, S. I., Shin, I., Schultz, P. G. and Endo, T. Probing the environment along the protein import pathways in yeast mitochondria by site-specific photocrosslinking. *PNAS* **94**, 485-490 (1997).
3. England, P. M., Lester, H. A. and Dougherty, D. A. Incorporation of esters into proteins: Improved synthesis of hydroxyacyl tRNAs. *Tet. Lett.* **40**, 6189-6192 (1999).
4. England, P. M., Lester, H. A. and Dougherty, D. A. Mapping disulfide connectivity using backbone ester hydrolysis. *Biochemistry* **38**, 14409-14415 (1999).
5. Koh, J. T., Cornish, V. W. and Schultz, P. G. An experimental approach to evaluating the role of backbone interactions in proteins using unnatural amino acid mutagenesis. *Biochemistry* **36**, 11314-11322 (1997).
6. Philipson, K. D., Gallivan, J. P., Brandt, G. S., Dougherty, D. A. and Lester, H. A. Incorporation of caged cysteine and caged tyrosine into a transmembrane segment of the nicotinic ACh receptor. *Am. J. Phys. Cell Phys* **281**, C195-C206 (2001).
7. Lopez-Otin, C. and Overall, C. M. Protease degradomics: A new challenge for proteomics. *Nat. Rev. Mol. Cell Biol.* **3**, 509-519 (2002).
8. Ripka, W. C. New thrombin inhibitors in cardiovascular disease. *Curr. Op. Chem. Biol.* **1**, 242-253 (1997).
9. Condra, J. H., Miller, M. D., Hazuda, D. J. and Emini, E. A. Potential new therapies for the treatment of HIV-1 infection. *Ann. Rev. Med.* **53**, 541-555 (2002).
10. Steiner, D. F. The proprotein convertases. *Curr. Op. Chem. Biol.* **2**, 31-39 (1998).
11. Thorsett, E. D. and Latimer, L. H. Therapeutic approaches to Alzheimer's disease. *Curr. Op. Chem. Biol.* **4**, 377-382 (2000).
12. Macfarlane, S. R., Seatter, M. J., Kanke, T., Hunter, G. D. and Plevin, R. Proteinase-activated receptors. *Pharm. Rev.* **53**, 245-282 (2001).
13. Chang, G., Spencer, R. H., Lee, A. T., Barclay, M. T. and Rees, D. C. Structure of the MscL homolog from *Mycobacterium tuberculosis*: a gated mechanosensitive ion channel. *Science* **282**, 2220-2226 (1998).
14. Dervan, P. B. Molecular recognition of DNA by small molecules. *Bioorg. Med. Chem.* **9**, 2215-2235 (2001).
15. Sakurai, T., Wong, E., Drescher, U., Tanaka, H. and Jay, D. G. Ephrin-A5 restricts topographically specific arborization in the chick retinotectal projection in vivo. *PNAS* **99**, 10795-10800 (2002).
16. Jay, D. G. and Sakurai, T. Chromophore-assisted laser inactivation (CALI) to elucidate cellular mechanisms of cancer. *Biochim. Biophys. Acta* **1424**, M39-M48 (1999).
17. Kumar, C. V. and Buranaprapuk, A. Site-specific photocleavage of proteins. *Angew. Chem. Int. Ed. Eng.* **36**, 2085-2087 (1997).
18. Kumar, C. V. et al. Photochemical protease: Site-specific photocleavage of hen egg lysozyme and bovine serum albumin. *PNAS* **95**, 10361-10366 (1998).
19. Kumar, C. V., Buranaprapuk, A., Sze, H. C., Jockusch, S. and Turro, N. J. Chiral protein scissors: High enantiomeric selectivity for binding and its effect on protein photocleavage efficiency and specificity. *PNAS* **99**, 5810-5815 (2002).
20. Baird, T., Wang, B. X., Lodder, M., Hecht, S. M. and Craik, C. S. Generation of active trypsin by chemical cleavage. *Tetrahedron* **56**, 9477-9485 (2000).

21. Wang, B. X., Brown, K. C., Lodder, M., Craik, C. S. and Hecht, S. M. Chemically mediated site-specific proteolysis. Alteration of protein-protein interaction. *Biochemistry* **41**, 2805-2813 (2002).
22. Wang, B. X. et al. Chemically mediated site-specific cleavage of proteins. *J. Am. Chem. Soc.* **122**, 7402-7403 (2000).
23. Ortells, M. O. and Lunt, G. G. Evolutionary history of the ligand-gated ion-channel superfamily of receptors. *Trends Neurosci.* **18**, 121-127 (1995).
24. Fu, D. X. and Sine, S. M. Asymmetric contribution of the conserved disulfide loop to subunit oligomerization and assembly of the nicotinic acetylcholine receptor. *J. Biol. Chem.* **271**, 31479-31484 (1996).
25. Rickert, K. W. and Imperiali, B. Analysis of the conserved glycosylation site in the nicotinic acetylcholine-receptor - potential roles in complex assembly. *Chem. Biol.* **2**, 751-759 (1995).
26. Criado, M., Sarin, V., Fox, J. L. and Lindstrom, J. Evidence that the acetylcholine binding-site is not formed by the sequence alpha-127-143 of the acetylcholine-receptor. *Biochemistry* **25**, 2839-2846 (1986).
27. Green, W. N. and Wanamaker, C. P. The role of the cystine loop in acetylcholine receptor assembly. *J. Biol. Chem.* **272**, 20945-20953 (1997).
28. Labarca, C. et al. Channel gating governed symmetrically by conserved leucine residues in the M2 domain of nicotinic receptors. *Nature* **376**, 514-6 (1995).
29. Sansom, M. S. P. Ion-channel gating - twist to open. *Curr. Biol.* **5**, 373-375 (1995).
30. Kearney, P. C., Zhang, H. Y., Zhong, W., Dougherty, D. A. and Lester, H. A. Determinants of nicotinic receptor gating in natural and unnatural side chain structures at the M2 9' position. *Neuron* **17**, 1221-1229 (1996).
31. Kearney, P. C. et al. Interactions of leucine residues at the 9' position of the M2 domain of the AChR probed using unnatural amino acid mutagenesis. *Biophys. J.* **70**, Tuam5-Tuam5 (1996).
32. Charnet, P., Labarca, C. and Lester, H. A. Structure of the gamma-less nicotinic acetylcholine-receptor - learning from omission. *Mol. Pharm.* **41**, 708-717 (1992).
33. Anand, R. et al. Reporter epitopes - a novel-approach to examine transmembrane topology of integral membrane-proteins applied to the alpha-1 subunit of the nicotinic acetylcholine-receptor. *Biochemistry* **32**, 9975-9984 (1993).
34. Knappik, A. and Pluckthun, A. An improved affinity tag based on the flag(r) peptide for the detection and purification of recombinant antibody fragments. *Biotechniques* **17**, 754-761 (1994).
35. Sato, M. H. and Wada, Y. Universal template plasmid for introduction of the triple-HA epitope sequence into cloned genes. *Biotechniques* **23**, 254-256 (1997).
36. Canfield, V. A., Norbeck, L. and Levenson, R. Localization of cytoplasmic and extracellular domains of Na,K-ATPase by epitope tag insertion. *Biochemistry* **35**, 14165-14172 (1996).
37. Bretzel, G. et al. Isolation of plasma membranes from *Xenopus* embryos. *Roux Arch. Dev. Biol.* **195**, 117-122 (1986).
38. Quick, M. W., Corey, J. L., Davidson, N. and Lester, H. A. Second messengers, trafficking-related proteins, and amino acid residues that contribute to the functional regulation of the rat brain GABA transporter GAT1. *J. Neurosci.* **17**, 2967-2979 (1997).
39. Corey, J. L. and Stallcup, M. R. The effect of glucocorticoid on the subcellular-localization, oligomerization, and processing of mouse mammary-tumor virus envelope protein precursor-Pr74. *Mol. Endocrinol.* **6**, 450-458 (1992).
40. Corey, J. L., Davidson, N., Lester, H. A., Brecha, N. and Quick, M. W. Protein-kinase-C modulates the activity of a cloned gamma-aminobutyric-acid transporter expressed in *Xenopus* oocytes via regulated subcellular redistribution of the transporter. *J. Biol. Chem.* **269**, 14759-14767 (1994).
41. Ivanina, T. et al. Phosphorylation by protein-kinase-A of RCK1 K^+ channels expressed in *Xenopus* oocytes. *Biochemistry* **33**, 8786-8792 (1994).
42. Dumont, J. N. Oogenesis in *Xenopus laevis* (Daudin).1. Stages of oocyte development in laboratory maintained animals. *J. Morphol.* **136**, 153-and (1972).
43. Keady, B., Attfield, K. and Hake, L. Identification and characterization of a CCA adding tRNA nucleotidyl transferase in Xenopus. *FASEB J.* **16**, A164-A164 (2002).
44. Hansske, F. and Cramer, F. Studies on structure of periodate oxidated ribonucleosides and ribonucleotides. *Carb. Res.* **54**, 75-84 (1977).

45. Sampson, J. R. and Saks, M. E. Selection of aminoacylated tRNAs front RNA libraries having randomized acceptor stem sequences: Using old dogs to perform new tricks. *Combi. Chem.* **267**, 384-410 (1996).
46. Thiry, M. Immunodetection of RNA on ultra-thin sections incubated with polyadenylate nucleotidyl transferase. *J. Histochem. Cytochem.* **41**, 657-665 (1993).
47. Petersson, E. J., Shahgholi, M., Lester, H. A. and Dougherty, D. A. MALDI-TOF mass spectrometry methods for evaluation of in vitro aminoacyl tRNA production. *RNA* **8**, 542-547 (2002).
48. Li, Z. J., Sun, Y. and Thurlow, D. L. RNA minihelices as model substrates for ATP/CTP:TRNA nucleotidyltransferase. *Biochem. J.* **327**, 847-851 (1997).
49. Green, W. N. Perspective - Ion channel assembly: Creating structures that function. *J. Gen. Phys.* **113**, 163-169 (1999).
50. Green, W. N. and Wanamaker, C. P. Formation of the nicotinic acetylcholine receptor binding sites. *J. Neurosci.* **18**, 5555-5564 (1998).
51. Palacin, M., Fernandez, E., Chillaron, J. and Zorzano, A. The amino acid transport system b(o,+) and cystinuria. *Mol. Memb. Biol.* **18**, 21-26 (2001).
52. Kellenberger, S. et al. Subunit stoichiometry of oligomeric membrane proteins: GABA(A) receptors isolated by selective immunoprecipitation from the cell surface. *Neuropharmacology* **35**, 1403-1411 (1996).
53. Nicke, A. et al. P2X(1) and P2X(3) receptors form stable trimers: a novel structural motif of ligand-gated ion channels. *EMBO J.* **17**, 3016-3028 (1998).
54. Nicke, A., Rettinger, J., Mutschler, E. and Schmalzing, G. Blue native page as a useful method for the analysis of the assembly of distinct combinations of nicotinic acetylcholine receptor subunits. *J. Rec. Sig. Trans. Res.* **19**, 493-507 (1999).
55. Hucho, F., Methfessel, C. and Watty, A. The role of subunit interfaces for the nicotinic acetylcholine receptor's allosterism. *J. Physiol. Paris* **92**, 85-88 (1998).
56. Watty, A., Weise, C., Dreger, M., Franke, P. and Hucho, F. The accessible surface of the nicotinic acetylcholine receptor - Identification by chemical modification and cross-linking with C-14-dimethyl suberimidate. *Eur. J. Biochem.* **252**, 222-228 (1998).
57. Leite, J. F., Blanton, M. P., Dougherty, D. A. and Lester, H. A. Identification of gating-dependent changes in photochemical labeling of the nicotinic acetylcholine receptor. *Biophys. J.* **82**, 181a-182a (2002).
58. Holmes, T. C., Fadool, D. A., Ren, R. B. and Levitan, I. B. Association of Src tyrosine kinase with a human potassium channel mediated by SH3 domain. *Science* **274**, 2089-2091 (1996).
59. Colledge, M. and Froehner, S. C. Signals mediating ion channel clustering at the neuromuscular junction. *Curr. Op. Neurobiol.* **8**, 357-363 (1998).
60. Sheng, M. and Kim, E. Ion channel associated proteins. *Curr. Op. Neurobiol.* **6**, 602-608 (1996).
61. Weber, P. J. A. and Beck-Sickinger, A. G. Comparison of the photochemical behavior of four different photoactivatable probes. *J. Pept. Res.* **49**, 375-383 (1997).
62. Mothes, W. et al. Molecular mechanism of membrane protein integration into the endoplasmic reticulum. *Cell* **89**, 523-533 (1997).
63. High, S. et al. Site-specific photocross-linking reveals that Sec61p and Tram contact different regions of a membrane-inserted signal sequence. *J. Biol. Chem.* **268**, 26745-26751 (1993).
64. Gallivan, J. P. *Ph.D. thesis* (California Institute of Technology, Pasadena, CA, 2000).
65. Brejc, K. et al. Crystal structure of an ACh-binding protein reveals the ligand-binding domain of nicotinic receptors. *Nature* **411**, 269-276 (2001).
66. Walker, C. S. et al. The T-superfamily of conotoxins. *J. Biol. Chem.* **274**, 30664-30671 (1999).
67. Kaerner, A. and Rabenstein, D. L. Stability and structure-forming properties of the two disulfide bonds of alpha-conotoxin GI. *Biochemistry* **38**, 5459-5470 (1999).
68. Brake, A. J., Wagenbach, M. J. and Julius, D. New structural motif for ligand-gated ion channels defined by an ionotropic ATP receptor. *Nature* **371**, 519-523 (1994).
69. North, R. A. P2X receptors: A third family of ligand-gated ion channels. *Br. J. Pharm.* **122**, U151-U151 (1997).
70. Newbolt, A. et al. Membrane topology of an ATP-gated ion channel (P2X receptor). *J. Biol. Chem.* **273**, 15177-15182 (1998).

71. North, R. A. and Surprenant, A. Pharmacology of cloned P2X receptors. *Ann. Rev. Pharm.* **40**, 563-580 (2000).
72. Curley, K. and Lawrence, D. S. Light-activated proteins. *Curr Opin. Chem. Biol.* **3**, 84-88 (1999).
73. Marriott, G. and Walker, J. W. Caged peptides and proteins: new probes to study polypeptide function in complex biological systems. *Trends Plant Sci.* **4**, 330-334 (1999).